

## MONTE CARLO STUDY OF THE STANDARD SU(2) HIGGS MODEL

W. LANGGUTH

*Institut für Theoretische Kernphysik der Universität Karlsruhe, Karlsruhe, FR Germany*

I. MONTVAY

*Deutsches Elektronen-Synchrotron DESY, Hamburg, FR Germany*

P. WEISZ\*

*II. Institut für Theoretische Physik der Universität Hamburg, Hamburg, FR Germany*

Received 23 December 1985

(Revised 14 April 1986)

The SU(2) Higgs model with scalar doublet field is numerically investigated on lattices with size between  $8^4$  and  $12^4$ . Masses and zero momentum couplings are determined at several points of the three-dimensional coupling parameter space. Particular interest is given to questions related to the order of the confinement-Higgs phase transition. It is shown that for non-perturbative scalar self-couplings numerical Monte Carlo calculations are possible in the region of weak gauge coupling approximately equal to the physical value in the standard SU(2)  $\otimes$  U(1) electroweak theory. Our first exploratory results in such a point on  $12^4$  lattice give a Higgs mass to W-mass ratio  $6.4 \pm 0.8$  and a Higgs-WW coupling roughly a factor 3 smaller than the tree-level value. The circumstances under which these numbers could have some phenomenological relevance are discussed. A possible strategy is outlined for future large scale Monte Carlo calculations in the strongly self-interacting standard Higgs model with weak gauge coupling.

### 1. Introduction

Our present understanding of high-energy elementary particle interactions is based to a large extent on quantum gauge field theories with spin- $\frac{1}{2}$  fermion matter fields. The prototype theories are QED with the electromagnetic U(1) gauge field and the spin- $\frac{1}{2}$  electron field, and QCD with SU(3) colour gauge field and triplets of spin- $\frac{1}{2}$  quarks. Quantum field theories with scalar matter fields are usually considered to be problematic or even inconsistent. An often asked question is: can elementary scalar particles exist?

In order to be able to answer this question one has to consider the regularized quantum field theory. In the case of gauge fields a natural cut-off is realized by a

\* Heisenberg foundation fellow.

finite space-time lattice [1], and the above question can be formulated by asking: is a lattice-regularized quantum gauge field theory with scalar matter fields mathematically consistent with a very small lattice spacing (i.e. with a cut-off much larger than the physical masses in the theory)? In the case of the simplest model with only scalar fields, namely the pure  $\phi^4$  model, it is almost exactly proven that an infinitely high cut-off is only possible in the trivial case of free fields, without physical interaction (for a review see, for instance [2]). If one requires a very large (but finite) cut-off, the value of the renormalized  $\phi^4$  coupling is restricted to a range with some small upper bound. Models without gauge fields have, of course, only academic interest, and the inclusion of gauge fields can change the situation.

A simple prototype gauge model with scalar matter fields is the “standard” SU(2) Higgs model with a scalar doublet, which is an important part of the standard SU(3)  $\otimes$  SU(2)  $\otimes$  U(1) theory. This and other similar Higgs models are well suited for numerical Monte Carlo studies (in fact, from the numerical point of view much simpler than gauge fields with fermions). Therefore, presently there is an increasing interest in the numerical investigation of Higgs models (for a recent review and references see [3]). The case of the standard SU(2) Higgs model is particularly simple, because the scalar doublet breaks the local gauge symmetry completely in the sense that no massless “photon” field is left over.

For zero gauge coupling the standard SU(2) Higgs model is identical to a four-component  $\phi^4$  model, which has presumably no non-trivial continuum limit. The inclusion of the gauge coupling could, in principle, produce a non-trivial critical point (for a non-trivial continuum limit) somewhere in the interior of the 3-dimensional coupling parameter space. (Besides the hopping parameter  $\kappa$  and scalar self-coupling  $\lambda$  of the pure  $\phi^4$  model the third bare coupling is  $\beta \equiv 4/g^2$ , which specifies the gauge field dynamics.) Recent numerical data on the correlation lengths and static energies [4–6], however, indicate that this is not probable. Moreover, the first Monte Carlo renormalization group (MCRG) study showed also no evidence for a non-trivial critical point at finite  $\beta$  [7]. This is not very surprising since, as a consequence of asymptotic freedom, the gauge coupling is always weak at small distances, even if it is strong at the scale of the physical masses. A non-trivial continuum limit in the standard SU(2) Higgs model can, however, exist at the critical line of the pure  $\phi^4$  component at  $\beta = \infty$ . This would be similar to the asymptotically free gauge theories with fermion matter fields, where the continuum limit is also at  $\beta = \infty$ .

The triviality of the pure  $\phi^4$  model implies that in the continuum limit the physics becomes independent of the self-coupling  $\lambda$  ( $\lambda$  is “irrelevant”). In the region  $0.1 \leq \lambda \leq \infty$ , which was up to now investigated by the Monte Carlo calculations, this  $\lambda$ -independence seems to be maintained also after the inclusion of the gauge coupling, if one considers the physical quantities, for fixed  $\beta$ , as a function of an appropriately chosen variable [4] (namely, the expectation value of the gauge invariant link variable). The  $\lambda$ -independence is an essentially non-perturbative

feature which can be exactly valid only for infinitely high cut-off. For any finite cut-off there is some range of sufficiently small self-coupling, where perturbation theory in  $\lambda$  is expected to be applicable. In this perturbative regime there is  $\lambda$ -dependence. The present Monte Carlo data in the Higgs model seem to be entirely within the strongly coupled non-perturbative region, where approximate  $\lambda$ -independence is true.

In the present paper we report on the results of an extensive numerical Monte Carlo study of the standard SU(2) Higgs model. We shall concentrate mainly on three new aspects: some zero four-momentum coupling constants of the physical Higgs- and W-bosons, a detailed comparison of  $8^4$  and  $12^4$  data from the point of view of finite size scaling and a high-statistics calculation in two points at weak gauge coupling roughly equal to the physical value in the SU(2)  $\otimes$  U(1) electroweak theory. The scalar self-coupling is always in the non-perturbative, approximately  $\lambda$ -independent, region. In the next section, after defining the notations, the obtained results for the masses and couplings on the  $8^4$  lattice will be summarized. Sect. 3 is devoted to the comparison of the behaviour near the phase transition on  $8^4$  and  $12^4$  lattices. As a part of this comparison, a finite size scaling analysis will also be carried out. In sect. 4 the Monte Carlo results at weak physical gauge coupling will be presented and discussed. A possible strategy for future Monte Carlo calculations on larger lattices and with higher statistics is outlined in an appendix. A recollection of the definitions about “renormalization group trajectories” or “curves of constant physics” is also included in the appendix. The last section is reserved for a few concluding remarks.

## 2. Masses and couplings

### 2.1. LATTICE ACTION

Throughout this paper we shall use for the lattice variables the notations of ref. [4]. In particular, the link variable for the gauge field will be denoted by  $U(x, \mu) \in \text{SU}(2)$  ( $x$  = lattice point,  $\mu$  = link direction), the Higgs field is specified by its length  $\rho_x \geq 0$  and by an SU(2) angular variable  $\alpha_x \in \text{SU}(2)$ . The lattice action in these variables can be written as

$$S_{\lambda, \beta, \kappa} = \beta \sum_{\text{P}} \left( 1 - \frac{1}{2} \text{Tr} U_{\text{P}} \right) + \sum_x \left\{ \rho_x^2 - 3 \log \rho_x + \lambda (\rho_x^2 - 1)^2 - \kappa \sum_{\mu > 0} \rho_{x+\hat{\mu}} \rho_x \text{Tr} (\alpha_{x+\hat{\mu}}^+ U(x, \mu) \alpha_x) \right\}. \quad (1)$$

Here  $\sum_{\text{P}}$  stands for a summation over positively oriented plaquettes. The integration measure corresponding to eq. (1) is  $d\rho_x d^3\alpha_x d^3U(x, \mu)$  (where  $d^3g$  denotes the

Haar-measure in  $SU(2)$ ). The peculiarity of the  $SU(2)$  doublet scalar field is, that its angular part is equivalent to the local gauge degree of freedom. Therefore, at any finite  $\beta$  it is possible to introduce, instead of the  $SU(2)$  link- and site-variables, a gauge invariant link variable

$$V(x, \mu) \equiv \alpha_{x+\hat{\mu}}^+ U(x, \mu) \alpha_x. \quad (2)$$

In terms of this, the lattice action is

$$S_{\lambda, \beta, \kappa} = \beta \sum_{\mathbf{P}} \left( 1 - \frac{1}{2} \text{Tr} V_{\mathbf{P}} \right) + \sum_x \left\{ \rho_x^2 - 3 \log \rho_x + \lambda (\rho_x^2 - 1)^2 - \kappa \sum_{\mu > 0} \rho_{x+\hat{\mu}} \rho_x \text{Tr} V(x, \mu) \right\}. \quad (3)$$

After performing the trivial integration over  $\alpha_x$ , the integration measure for eq. (3) is  $d\rho_x d^3V(x, \mu)$ .

In the limit  $\lambda \rightarrow \infty$  the length of the Higgs field is frozen to unity, and the action in eq. (1) can be replaced by

$$S_{\lambda=\infty, \beta, \kappa} = \beta \sum_{\mathbf{P}} \left( 1 - \frac{1}{2} \text{Tr} U_{\mathbf{P}} \right) - \kappa \sum_{x, \mu > 0} \text{Tr} (\alpha_{x+\hat{\mu}}^+ U(x, \mu) \alpha_x), \quad (4)$$

whereas, instead of eq. (3) one can use

$$S_{\lambda=\infty, \beta, \kappa} = \beta \sum_{\mathbf{P}} \left( 1 - \frac{1}{2} \text{Tr} V_{\mathbf{P}} \right) - \kappa \sum_{x, \mu > 0} \text{Tr} V(x, \mu). \quad (5)$$

## 2.2. MONTE CARLO MEASUREMENT OF THE MASSES AND COUPLINGS

The masses are extracted in the Monte Carlo calculation from the exponential decay of two-point correlation functions. In the Higgs-boson (scalar, isoscalar) channel we used the diagonal correlations of the quantities

$$h_x = \begin{cases} h_x^{(1)} \equiv \rho_x, \\ h_x^{(2)} \equiv \text{Tr} V(x, \mu), & (\mu = 1, 2, 3, 4) \\ h_x^{(3)} \equiv \rho_{x+\hat{\mu}} \rho_x \text{Tr} V(x, \mu), & (\mu = 1, 2, 3, 4) \end{cases}. \quad (6)$$

In the W-boson (vector, isovector) channel correlations of

$$w_{x r \mu} = \begin{cases} w_{x r \mu}^{(1)} \equiv \text{Tr} (\tau_r V(x, \mu)) \\ w_{x r \mu}^{(2)} \equiv \rho_{x+\hat{\mu}} \rho_x \text{Tr} (\tau_r V(x, \mu)) \end{cases} \quad (7)$$

were considered ( $\tau$ , denotes a Pauli-matrix). The Monte Carlo calculations show that the three Higgs-boson and two W-boson channels are strongly correlated, that is, the masses determined in the same channel by different quantities deviate from each other much less than the individual statistical errors.

The zero momentum couplings are usually defined on the lattice in such a way that no multiplicative wave function renormalization is left over. In the case of the  $n$ -Higgs-boson coupling  $\Lambda_{nH}$  the definition is (for  $n \geq 3$ ):

$$a^{4-2n}\Lambda_{nH} \equiv \frac{(1/N)\sum_{x_1 \dots x_n} \langle h_{x_1} \dots h_{x_n} \rangle^c}{\left[ (1/N)\sum_{x_1 x_2} \langle h_{x_1} h_{x_2} \rangle^c \right]^{n/2}}. \quad (8)$$

Here  $a$  is the lattice spacing,  $N$  the number of lattice sites,  $\langle \dots \rangle^c$  means connected part of the expectation value, and  $h_x$  is one of the interpolating fields for the Higgs boson in eq. (6). Multiplying eq. (8) by the appropriate power  $(am_H)^{2n-4}$  of the Higgs boson mass, one obtains the dimensionless quantity

$$l_{nH} \equiv m_H^{2n-4} \Lambda_{nH}. \quad (9)$$

Since the coupling  $\Lambda_{nH}$  is defined off-mass-shell (at  $p=0$ ), its value is not independent of the choice of the interpolating field  $h_x$ . Only the corresponding on mass shell coupling is independent, and has an immediate physical meaning. The best estimate of the physical couplings of some particular state can be obtained by using the correlations of those quantities, which are most dominated by that state.

Let us note that the zero momentum coupling  $\lambda_{nH}$  usually considered in weak coupling perturbation theory is not exactly the same as  $\Lambda_{nH}$ , because it is ‘‘truncated’’ by  $n$  propagators (and not by  $\frac{1}{2}n$ ). One can, however, consider ratios of  $\Lambda_{nH}$ , which coincide with the corresponding ratios of  $\lambda_{nH}$ , for instance,

$$\rho_{(3)nH} \equiv \frac{\Lambda_{nH}}{|\Lambda_{3H}|^{n/3}} = \frac{\lambda_{nH}}{|\lambda_{3H}|^{n/3}}. \quad (10)$$

The Higgs-WW coupling is decisive for the decay of the Higgs boson, if it is heavier than twice the W-boson. On the lattice, in analogy to eq. (8), the zero four-momentum Higgs-WW coupling can be defined as

$$a^{-2}\Lambda_{HWW} \equiv \frac{(1/N)\sum_{x_1 x_2 x_3} \sum_{r\mu} \langle h_{x_1} w_{x_2 r\mu} w_{x_3 r\mu} \rangle^c}{\left[ (1/N)\sum_{x_1 x_2} \langle h_{x_1} h_{x_2} \rangle^c \right]^{1/2} \left[ (1/N)\sum_{x_2 x_3} \sum_{r\mu} \langle w_{x_2 r\mu} w_{x_3 r\mu} \rangle^c \right]}. \quad (11)$$

Here  $w_{x r\mu}$  is one of the interpolating fields for the W-boson in eq. (7). A dimensionless quantity corresponding to  $\Lambda_{HWW}$  is, for instance,

$$l_{HWW} \equiv m_H m_W \Lambda_{HWW}. \quad (12)$$

The numerical problem in the calculation of the zero momentum couplings in eqs. (8), (11) is the strong cancellation involved by taking the connected part. In order to see this more explicitly, let us consider, for instance, eq. (8) in more detail. Let us denote the lattice average of the interpolating field  $h_x$  by  $\bar{h}$ :

$$\bar{h} = \frac{1}{N} \sum_x h_x. \quad (13)$$

Note that  $\bar{h}$  is proportional to the zero momentum component of  $h_x$ . In terms of  $\bar{h}$  the connected part in eq. (8) is:

$$\frac{1}{N} \sum_{x_1 \dots x_n} \langle h_{x_1} \dots h_{x_n} \rangle^c = N^{n-1} \langle \bar{h}^n \rangle^c. \quad (14)$$

Therefore we have ( $n \geq 3$ ):

$$a^{4-2n} \Lambda_{nH} = N^{n/2-1} \frac{\langle \bar{h}^n \rangle^c}{\{ \langle \bar{h}^2 \rangle^c \}^{n/2}}. \quad (15)$$

The cancellation involved in eqs. (14) and (15) is displayed by the large factors given by the powers of the number of lattice points ( $N$ ).

In order to obtain  $\langle \bar{h}^n \rangle^c$ , one can proceed (at least) in two different practical ways. The first is to calculate  $\langle \bar{h}^n \rangle$  in a straightforward way for different binnings of the sweeps and determine the connected part  $\langle \bar{h}^n \rangle^c$  from the sweeps belonging to one bin. This immediately gives an estimate of the errors of  $\langle \bar{h}^n \rangle^c$ , too. Another possible way is to measure the probability distribution  $w(\bar{h}, \bar{h} + \Delta\bar{h})$  of the values of  $\bar{h}$  during the updating. The expectation value of  $\bar{h}^n$  is, obviously:

$$\langle \bar{h}^n \rangle = \sum_b \bar{h}_b^n w(\bar{h}_b, \bar{h}_b + \Delta\bar{h}_b). \quad (16)$$

Here the sum goes over the bins  $(\bar{h}, \bar{h} + \Delta\bar{h})$  for the values of  $\bar{h}$ . Of course, this equation is exact only in the limit  $\Delta\bar{h} \rightarrow 0$ . The error estimate for  $\langle \bar{h}^n \rangle^c$  is somewhat cumbersome in this case, because one has to consider subsets of the performed sweeps, and obtain the probability distribution  $w$  and the value of  $\langle \bar{h}^n \rangle^c$  in these subsets.

### 2.3. MONTE CARLO RESULTS ON $8^4$ AT $\beta = 2.3$

In the Monte Carlo simulation at  $\beta = 2.3$  we mainly investigated the immediate vicinity of the confinement-Higgs phase transition. In the present section we discuss the results for the masses and couplings obtained on the  $8^4$  lattice. Some similar results on the  $12^4$  lattice were already published in ref. [6], and the comparison of  $8^4$

and  $12^4$  from the point of view of the order of the phase transition will be the subject of the next section. Most of the points in the coupling parameter space are at  $\lambda = \infty$  and  $\lambda = 1.0$ , but we have also a few points at  $\lambda = 0.1$ .

The Monte Carlo calculation was performed by using the Metropolis method with 6 hits per gauge invariant variables in the actions in eq. (3) and eq. (5). From previous experience [4] we know, that at such  $\beta$ -values the inclusion of the gauge degrees of freedom is unnecessary. The site- and link-variables were updated in alternating sweeps in a randomly changing order. The acceptance rate was kept near  $\frac{1}{3}$  per hit. We always used the full  $SU(2)$  group on the links. The boundary conditions were periodic. The total number of double-sweeps was typically  $(8-10) \times 10^4$  per point. The statistical errors were estimated by binning the data in bins of length  $2^k$  ( $k = 0, 1, 2, \dots$ ), and estimating the standard deviations from the bin averages. Right on top of the phase transition very long time correlations were observed (sometimes in the order of 10 000 sweeps), therefore the error estimates did not always saturate with the increasing bin length. In these points the errors may be underestimated. Away from the phase transition the time correlations are considerably smaller and, therefore, the statistical error estimates are reliable.

The measured masses in the W-boson ( $am_W$ ) and Higgs boson ( $am_H$ ) channels and some average quantities like the average link  $L$ , average  $\rho$ -link  $R$ , average plaquette  $P$ , average length  $\rho$  and average action per site  $s$  are collected in table 1. The definitions of the average quantities are

$$\begin{aligned}
 L &= \left\langle \frac{1}{2} \text{Tr} V(x, \mu) \right\rangle, & R &= \left\langle \frac{1}{2} \rho_{x+\hat{\mu}} \rho_x \text{Tr} V(x, \mu) \right\rangle, \\
 P &= \left\langle 1 - \frac{1}{2} \text{Tr} V_P \right\rangle, & \rho &= \langle \rho_x \rangle, \\
 s &= 6\beta \left\langle 1 - \frac{1}{2} \text{Tr} V_P \right\rangle + \left\langle \rho_x^2 - 3 \log \rho_x + \lambda (\rho_x^2 - 1)^2 \right\rangle + 8\kappa \left\langle 1 - \frac{1}{2} \rho_{x+\hat{\mu}} \rho_x \text{Tr} V(x, \mu) \right\rangle.
 \end{aligned} \tag{17}$$

The correlations could always be determined up to the largest distance ( $d_{\max} = 4$ ), therefore mass estimates could be obtained from all distances by using the formula

$$am^{(d)} = \frac{1}{d_{\max} - d} \log \left\{ \frac{C_d}{C_{d_{\max}}} + \sqrt{\left( \frac{C_d}{C_{d_{\max}}} \right)^2 - 1} \right\} \quad (0 \leq d < d_{\max}), \tag{18}$$

where  $C_d$  is the correlation at distance  $d$ . Usually,  $d = 2, 3$  gives already consistent results, that is, these distances are reasonably well dominated by the lowest state. At some points, for instance very near to the phase transition in the W-boson channels,  $am^{(3)}$  was still definitely smaller than  $am^{(2)}$ . In such cases the time extension of the

TABLE I  
The W-boson mass ( $am_W$ ) and Higgs boson mass ( $am_H$ ) in lattice units  
on  $8^4$  lattice at  $\beta = 2.3$

| $\lambda$ | $\kappa$ | $am_W$   | $am_H$   | $L$        | $R$        | $P$        | $\rho$     | $s$       |
|-----------|----------|----------|----------|------------|------------|------------|------------|-----------|
| $\infty$  | 0.380    | 1.40(13) | 1.35(14) | 0.2325(2)  |            | 0.3930(1)  |            | 8.756(2)  |
| $\infty$  | 0.385    | 1.11(14) | 0.68(7)  | 0.2403(4)  |            | 0.3922(1)  |            | 8.753(3)  |
| $\infty$  | 0.388    | 0.94(11) | 0.55(4)  | 0.2455(6)  |            | 0.3915(2)  |            | 8.744(5)  |
| $\infty$  | 0.390    | 0.78(9)  | 0.45(5)  | 0.2504(6)  |            | 0.3907(2)  |            | 8.729(4)  |
| $\infty$  | 0.392    | 1.16(12) | 0.45(4)  | 0.2574(10) |            | 0.3894(3)  |            | 8.702(7)  |
| $\infty$  | 0.393    | 0.86(8)  | 0.36(4)  | 0.2601(10) |            | 0.3889(2)  |            | 8.694(6)  |
| $\infty$  | 0.394    | 0.76(8)  | 0.33(3)  | 0.2638(10) |            | 0.3882(5)  |            | 8.677(14) |
| $\infty$  | 0.395    | 0.68(6)  | 0.32(3)  | 0.2690(12) |            | 0.3871(6)  |            | 8.653(14) |
| $\infty$  | 0.396    | 0.66(6)  | 0.39(4)  | 0.2741(13) |            | 0.3858(4)  |            | 8.633(12) |
| $\infty$  | 0.397    | 0.66(6)  | 0.39(4)  | 0.2787(11) |            | 0.3849(6)  |            | 8.60(2)   |
| $\infty$  | 0.398    | 0.53(7)  | 0.41(3)  | 0.2863(10) |            | 0.3833(3)  |            | 8.561(6)  |
| $\infty$  | 0.400    | 0.66(7)  | 0.54(7)  | 0.2933(7)  |            | 0.3822(2)  |            | 8.536(4)  |
| $\infty$  | 0.402    | 0.56(5)  | 0.56(7)  | 0.2992(6)  |            | 0.3814(1)  |            | 8.518(4)  |
| $\infty$  | 0.405    | 0.51(5)  | 0.91(10) | 0.3071(4)  |            | 0.3804(1)  |            | 8.494(3)  |
| $\infty$  | 0.410    | 0.53(4)  | 0.82(7)  | 0.3214(3)  |            | 0.3784(1)  |            | 8.448(2)  |
| 1.0       | 0.3036   | 0.64(9)  | 0.32(3)  | 0.2576(16) | 0.3585(25) | 0.3871(3)  | 1.1254(6)  | 8.406(9)  |
| 1.0       | 0.3038   | 0.61(6)  | 0.29(3)  | 0.2701(18) | 0.3780(29) | 0.3847(3)  | 1.1301(7)  | 8.332(9)  |
| 1.0       | 0.3039   | 0.74(6)  | 0.33(3)  | 0.2666(18) | 0.3724(29) | 0.3857(4)  | 1.1288(7)  | 8.357(10) |
| 1.0       | 0.3040   | 0.58(6)  | 0.33(3)  | 0.2720(20) | 0.3809(31) | 0.3845(3)  | 1.1309(7)  | 8.322(10) |
| 1.0       | 0.3041   | 0.62(6)  | 0.31(3)  | 0.2678(21) | 0.3743(33) | 0.3855(3)  | 1.1293(8)  | 8.352(10) |
| 1.0       | 0.3042   | 0.69(8)  | 0.31(3)  | 0.2727(21) | 0.3821(33) | 0.3846(3)  | 1.1312(8)  | 8.325(10) |
| 1.0       | 0.3045   | 0.67(7)  | 0.46(4)  | 0.2790(13) | 0.3921(21) | 0.3831(3)  | 1.1336(5)  | 8.283(9)  |
| 1.0       | 0.3070   | 0.53(5)  | 0.68(4)  | 0.3015(8)  | 0.4283(13) | 0.3798(2)  | 1.1428(3)  | 8.171(4)  |
| 0.1       | 0.194    | 0.55(5)  | 0.25(3)  | 0.2882(46) | 0.683(13)  | 0.3809(5)  | 1.4245(39) | 7.360(17) |
| 0.1       | 0.196    | 0.53(5)  | 0.86(3)  | 0.3485(6)  | 0.8710(20) | 0.3733(2)  | 1.4800(6)  | 7.059(4)  |
| 0.1       | 0.250    | 1.12(3)  | 2.14(6)  | 0.7475(2)  | 3.5955(18) | 0.31235(4) | 2.1778(3)  | 3.481(2)  |

The average quantities  $L$ ,  $R$ ,  $P$ ,  $\rho$  and  $s$  are defined in eq. (17). The statistical errors in the last numerals are given in parentheses.

$8^4$  lattice is obviously too small for a good mass estimate. In any case, the masses in table 1 can be taken as upper limits. From this point of view, the situation on the  $12^4$  lattice is much better, because there  $am^{(d)}$  could be taken with  $d_{\max} = 6$ .

The masses of, respectively, the W-boson and Higgs boson are shown in fig. 1a and 1b as a function of the link expectation value  $L$ . The figures show that the approximate universality observed in ref. [4] is good within the considerably smaller errors of the present calculation, too. In particular, the universality is not worse in the Higgs channel than in the W-channel, quite contrary to the weak coupling perturbation theoretic expectation. The only point where a deviation from universality of the Higgs mass may be indicated by the data is at ( $\lambda = 0.1$ ,  $\kappa = 0.194$ ). This point, however, is in the region of the phase transition, where metastability can be observed (see next section). Since the metastability is strongly volume dependent,



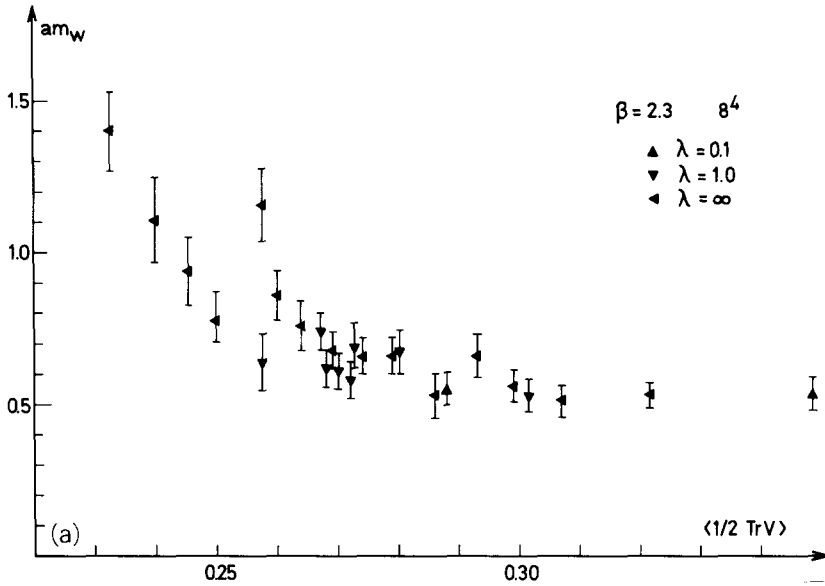


Fig. 1a. The W-boson mass in lattice units ( $am_W$ ) as a function of the link expectation value  $L = \langle \frac{1}{2} \text{Tr} V(x, \mu) \rangle$  for different  $\lambda$ -values at  $\beta = 2.3$ , on  $8^4$  lattice.

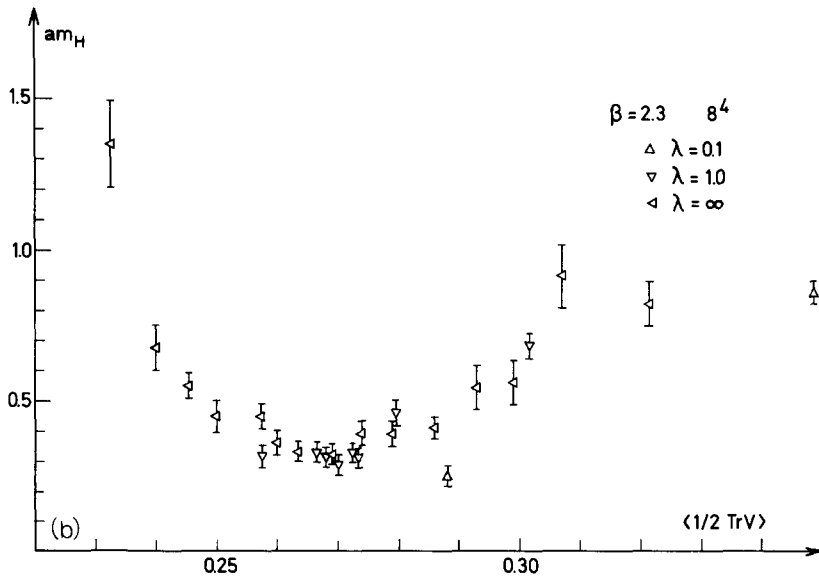


Fig. 1b. The same as fig. 1a, for the Higgs-boson mass ( $am_H$ ).

such points are not characteristic to the infinite volume limit. (In the next section we shall also see that the metastability effects mainly the Higgs mass.)

The new data confirm the qualitative behaviour of the masses seen in ref. [4]. The  $W$ -mass is large below the phase transition. Just below the phase transition and in the phase transition region itself it drops rapidly to a value about  $am_W \simeq 0.5$  and stays practically constant, with a rather slow increase, above the phase transition. The Higgs mass  $am_H$  is greater or equal than  $am_W$  in the Higgs phase (i.e. above the phase transition), and smaller than  $am_W$  in the confinement phase (i.e. below the phase transition). Inside the phase transition region  $am_H$  has a rather small value ( $am_H \simeq 0.3$  on the  $8^4$  lattice). All these features are in good agreement with the recent findings of the Aachen-Graz group [8] at slightly different parameter values.

For some technical reasons, the zero momentum couplings were not determined in every point. We have only two points with full statistics for the  $n$ -Higgs couplings ( $nH$ ;  $n = 3, 4, 5, 6$ ) and for the Higgs-WW coupling (HWW). As discussed in sect. 2, these quantities are, in general, difficult to calculate with an acceptable statistical error, because the extraction of the connected parts from the correlation functions involves a high degree of cancellation. From this point of view the HWW coupling is somewhat more favourable than the 3H coupling. The 4H and 5H couplings are, of course, even more difficult, and the 6H coupling is not measurable at all within our statistics.

The two points where the couplings were determined are (always with  $\beta = 2.3$ ):

$$\text{point A: } \lambda = 1.0, \quad \kappa = 0.307; \quad \text{point B: } \lambda = 0.1, \quad \kappa = 0.196. \quad (19)$$

We tried both methods for the extraction of the connected parts discussed in sect. 2. The probability distribution  $w$  for the average values was collected in 10000 bins. The two ways gave for the couplings identical results within errors. The distributions of the averages  $\rho$ ,  $L$  and  $R$  at point A are shown in figs. 2a–2c. The results for the  $nH$  couplings  $\Lambda_{nH}^{(j)}$  obtained by using the interpolating fields  $h^{(j)}$ , ( $j = 1, 2, 3$ ) in eq. (6) are:

$$\begin{aligned} \text{A: } & \begin{cases} a^{-2}\Lambda_{3H}^{(1)} = -5.6 \pm 2.5, & a^{-4}\Lambda_{4H}^{(1)} = (2.9 \pm 1.6) \times 10^2, & a^{-6}\Lambda_{5H}^{(1)} = (-1.5 \pm 1.3) \times 10^4 \\ a^{-2}\Lambda_{3H}^{(2)} = -11.0 \pm 5.5, & a^{-4}\Lambda_{4H}^{(2)} = (9.8 \pm 4.7) \times 10^2, & a^{-6}\Lambda_{5H}^{(2)} = (-4.7 \pm 4.5) \times 10^4, \\ a^{-2}\Lambda_{3H}^{(3)} = -9.4 \pm 5.2, & a^{-4}\Lambda_{4H}^{(3)} = (9.4 \pm 4.5) \times 10^2, & a^{-6}\Lambda_{5H}^{(3)} = (-3.3 \pm 4.2) \times 10^4 \end{cases} \\ \text{B: } & \begin{cases} a^{-2}\Lambda_{3H}^{(1)} = -6.9 \pm 3.2, & a^{-4}\Lambda_{4H}^{(1)} = (4.3 \pm 1.9) \times 10^2, & a^{-6}\Lambda_{5H}^{(1)} = (-1.1 \pm 0.5) \times 10^5 \\ a^{-2}\Lambda_{3H}^{(2)} = -12.6 \pm 5.0, & a^{-4}\Lambda_{4H}^{(2)} = (8.5 \pm 2.7) \times 10^2, & a^{-6}\Lambda_{5H}^{(2)} = (-6.0 \pm 8.8) \times 10^4, \\ a^{-2}\Lambda_{3H}^{(3)} = -7.8 \pm 4.3, & a^{-4}\Lambda_{4H}^{(3)} = (5.0 \pm 2.6) \times 10^2, & a^{-6}\Lambda_{5H}^{(3)} = (-4.5 \pm 7.7) \times 10^4 \end{cases} \end{aligned} \quad (20)$$

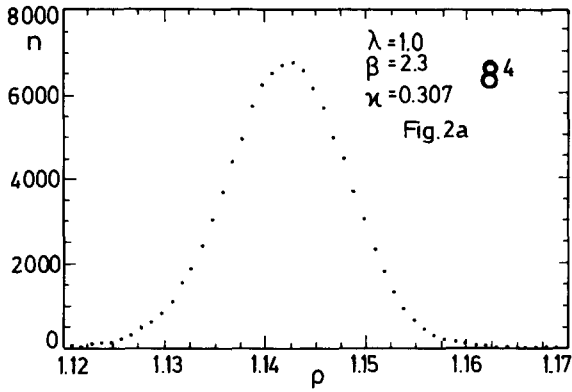


Fig. 2a. The distribution of average field length ( $\rho$ ) in the point ( $\lambda = 1$ ,  $\beta = 2.3$ ,  $\kappa = 0.307$ ) during the updating.

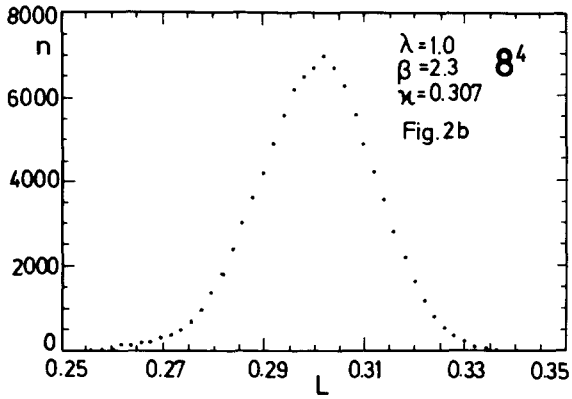


Fig. 2b. The same as fig. 2a for the average link ( $L$ ).

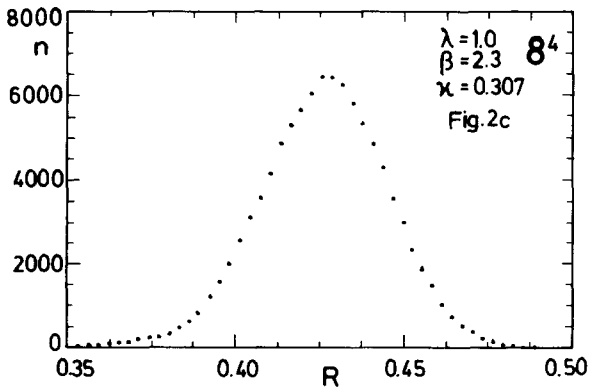


Fig. 2c. The same as fig. 2a for the average  $\rho$ -link ( $R$ ) defined in eq. (17).

The errors are, unfortunately, still very large. The dependence on the choice of the interpolating field is reduced for the ratios defined in eq. (10). For instance, for the 3H and 4H couplings we have:

$$\begin{aligned} \text{A: } & \rho_{(3)4\text{H}}^{(1)} \approx 28.9, & \rho_{(3)4\text{H}}^{(2)} \approx 39.8, & \rho_{(3)4\text{H}}^{(3)} \approx 47.6, \\ \text{B: } & \rho_{(3)4\text{H}}^{(1)} \approx 33.0, & \rho_{(3)4\text{H}}^{(2)} \approx 29.0, & \rho_{(3)4\text{H}}^{(3)} \approx 32.1. \end{aligned} \quad (21)$$

Let us remark that in a recent paper [9] the zero-momentum renormalized  $\phi^4$  coupling in the one- and four-component  $\phi^4$  model was calculated from the probability distribution  $w$  of averages. The aim was to obtain an upper bound on the Higgs boson mass. Since the Monte Carlo calculation in ref. [9] has only a rather limited statistics (42 000 sweeps on  $4^4$  and 14 000 sweeps on  $6^4$  lattice), it seems to us that the quoted small errors are incorrect. (The way of estimating the errors is not discussed in the paper.)

The HWW coupling has smaller errors, and its dependence on the choice of  $h^{(j)}$ , ( $j = 1, 2, 3$ ) is negligible compared to the statistical errors, therefore we averaged this coupling over  $j$ . The influence of the choice of the interpolating field for the W-boson  $w^{(k)}$ , ( $k = 1, 2$ ) in eq. (7) is more significant:

$$\begin{aligned} \text{A: } & a^{-2}\Lambda_{\text{HWW}}^{(k=1)} = 1.66 \pm 0.28, & a^{-2}\Lambda_{\text{HWW}}^{(k=2)} = 2.56 \pm 0.24, \\ \text{B: } & a^{-2}\Lambda_{\text{HWW}}^{(k=1)} = 1.60 \pm 0.21, & a^{-2}\Lambda_{\text{HWW}}^{(k=2)} = 3.34 \pm 0.27. \end{aligned} \quad (22)$$

One can see that, within the present errors, the couplings show no dramatic  $\lambda$ -dependence. (Note that, according to table 1, the link expectation values are only approximately equal in the two points.) Of course, the large errors of the  $n\text{H}$  couplings, unfortunately, prevent any firm conclusions for the moment. A dedicated high statistics numerical study of the couplings clearly deserves future attention.

### 3. $8^4$ versus $12^4$ lattice

#### 3.1. QUESTIONING THE ORDER OF THE PHASE TRANSITION

The order of the confinement-Higgs phase transition is an important issue in the standard SU(2) Higgs model. In particular, the existence and properties of the continuum limit at the  $\beta = \infty$  critical points may depend also on the order of the phase transition at finite  $\beta$ . In the case of a second-order phase transition line in the  $\lambda = \text{const}$  planes the correlation lengths are infinite along this line. This allows for the expected exponential rise of the correlation lengths  $\exp(\text{const } \beta)$  along the renormalization group trajectories (RGT's) going to the critical point at  $\beta = \infty$  near the phase transition line. (For a recollection of the definition of renormalization

group trajectories or “curves of constant physics” in a lattice field theory with several coupling parameters see appendix A.1.) The picture of the RGT’s in the  $(\beta, \kappa)$ -plane could then qualitatively be given by fig. 3a. In this case the analogy between the  $SU(2)$  gauge theory with scalar doublet matter field (for  $\lambda = \text{fixed}$ ) and an  $SU(2)$  gauge theory with a spin- $\frac{1}{2}$  fermion doublet is almost perfect, since for fermions there is also a second-order critical line at zero fermion mass. If, however, the phase transition line in the Higgs model is first order everywhere except for the endpoint at  $\beta = \infty$  (where it is second order), then there is no reason for the correlation lengths to diverge for finite  $\beta$ . If the maximum of the correlation lengths does not increase sufficiently fast for  $\beta \rightarrow \infty$ , then the (approximate) RGT’s can not reach the critical point at  $\beta = \infty$ : they end on the discontinuity at the first-order line for some finite correlation length, as it is shown by fig. 3b. In this case the critical point at  $\beta = \infty$  is likely to be trivial (i.e. equivalent to the pure gauge theory

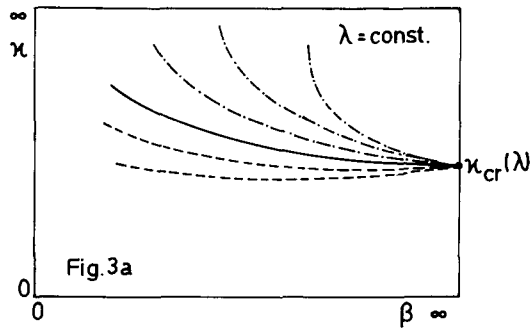


Fig. 3a. The schematic picture of RGT’s in a  $\lambda = \text{const}$  plane in the case of a second-order phase transition line (full line). The dashed-dotted lines are the RGT’s in the Higgs-phase, the dashed ones the RGT’s in the confinement phase. The correlation lengths diverge for  $\beta \rightarrow \infty$ .

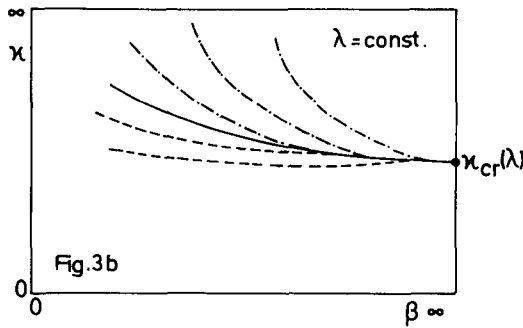


Fig. 3b. The same as fig. 3a in the case of a first-order phase transition line (full line) ending in a second order point  $\beta = \infty, \kappa_{cr}(\lambda)$ , provided that the correlation length along the phase transition line is not increasing fast enough for  $\beta \rightarrow \infty$ .

in the confinement phase and to a free theory of massive bosons in the Higgs phase). Therefore, in the case of a first-order phase transition line, the sufficiently fast increase of the maximum correlation length along the line is a non-trivial requirement for the existence of a non-trivial continuum limit in the  $\beta = \infty$  critical point.

Recent high-statistics Monte Carlo results imply [8] that for small  $\lambda$  the confinement-Higgs phase transition is strongly first order. For increasing  $\lambda$  and/or increasing  $\beta$  it is observed that the first-order transition becomes weaker. Therefore, in principle, it is possible that on the phase transition surface there is a tricritical line and beyond this the transition is second order. However, as far as the  $\lambda$ -dependence is concerned, this does not seem to happen for  $\beta = 2.3$ , because of the two-state signal observed on a  $12^4$  lattice [6]. In this section we want to elaborate on the question of the two-state signal by presenting more details of the  $12^4$  calculation and also by comparing the behaviour near the phase transition on  $8^4$  and  $12^4$  lattices.

The investigation of the volume dependence is important, because a statement about the order is, in fact, a statement about the volume dependence for very large volumes. Mathematically speaking the distinction refers only to the infinite volume limit but, of course, the qualitatively different features normally set in on finite, but large enough, lattices. In the case of an expected first-order phase transition, however, one has to be aware of the peculiar volume dependence implied by the metastability of the two phases. On a finite lattice the first-order phase transition is “rounded-off” and there is a finite range of parameters (in our case, for fixed  $\lambda$  and  $\beta$ , a range of  $\kappa$ ), where the system shows metastability and flips between the two phases during the Monte Carlo iteration. This, of course, implies long-range correlations. For increasing volume the range of metastability in  $\kappa$  shrinks to zero and also moves towards the discontinuity point for infinite volume. (For a systematic approach of the description of finite size effects in phase transitions see the recent paper of Brézin and Zinn-Justin [10], where references to previous work can also be found.) As a consequence, the observation of long-range correlations in a finite volume does not necessarily mean second-order phase transition. In the case of a first-order phase transition, for fixed parameter values which do not coincide with the discontinuity, the long-range correlation disappears once the volume is large enough. At a second-order phase transition the region of large correlation lengths has a finite limiting extent. In other words, for a first order phase transition there are strong finite size effects in the region of metastability. Therefore the metastability region has to be avoided if one wants to draw conclusions about the properties of the infinite volume system.

### 3.2. TWO-STATE SIGNALS

The Monte Carlo calculation on the  $12^4$  lattice was performed in the same way as on  $8^4$  (the number of sweeps was  $(8-12) \times 10^4$  per point). Some results on  $12^4$  were

TABLE 2  
Summary of the masses and average quantities obtained  
on  $12^4$  lattice at  $\beta = 2.3$

| $\lambda$ | $\kappa$ | $am_W$   | $am_H$  | $L$        | $R$        | $P$         | $\rho$    | $s$       |
|-----------|----------|----------|---------|------------|------------|-------------|-----------|-----------|
| $\infty$  | 0.390    | 1.26(6)  | 0.40(2) | 0.2485(2)  |            | 0.39126(8)  |           | 8.744(2)  |
| $\infty$  | 0.392    | 0.82(6)  | 0.35(2) | 0.2535(3)  |            | 0.39047(9)  |           | 8.729(2)  |
| $\infty$  | 0.394    | 0.70(8)  | 0.35(4) | 0.2599(4)  |            | 0.38937(15) |           | 8.706(4)  |
| $\infty$  | 0.395    | 0.73(6)  | 0.21(2) | 0.2677(8)  |            | 0.3876(3)   |           | 8.664(7)  |
| $\infty$  | 0.396    | 0.47(3)  | 0.24(2) | 0.2735(6)  |            | 0.3864(4)   |           | 8.629(9)  |
| $\infty$  | 0.397    | 0.31(4)  | 0.26(2) | 0.2783(6)  |            | 0.3854(3)   |           | 8.610(8)  |
| $\infty$  | 0.398    | 0.45(4)  | 0.44(3) | 0.2856(4)  |            | 0.38377(14) |           | 8.570(4)  |
| $\infty$  | 0.400    | 0.48(2)  | 0.53(4) | 0.2931(3)  |            | 0.38253(11) |           | 8.544(4)  |
| $\infty$  | 0.410    | 0.51(2)  | 0.79(3) | 0.3214(2)  |            | 0.37860(5)  |           | 8.450(2)  |
| 1.0       | 0.3020   | 1.18(23) | 0.63(7) | 0.2378(4)  | 0.3275(6)  | 0.39125(9)  | 1.1177(2) | 8.520(3)  |
| 1.0       | 0.3041   | 0.53(4)  | 0.16(1) | 0.2651(14) | 0.3702(21) | 0.3863(3)   | 1.1284(5) | 8.373(10) |
| 1.0       | 0.3042   | 0.52(5)  | 0.17(2) | 0.2682(14) | 0.3750(21) | 0.3855(3)   | 1.1295(5) | 8.352(8)  |
| 1.0       | 0.3045   | 0.40(3)  | 0.18(2) | 0.2751(14) | 0.3860(22) | 0.3840(3)   | 1.1322(5) | 8.304(9)  |
| 1.0       | 0.3050   | 0.39(3)  | 0.35(4) | 0.2865(6)  | 0.4039(10) | 0.3821(2)   | 1.1365(3) | 8.244(4)  |
| 1.0       | 0.3070   | 0.50(3)  | 0.57(5) | 0.3030(4)  | 0.4308(6)  | 0.37973(6)  | 1.1434(2) | 8.167(2)  |
| 1.0       | 0.3100   | 0.52(3)  | 0.78(4) | 0.3229(3)  | 0.4639(5)  | 0.37720(6)  | 1.1520(1) | 8.076(2)  |

already published in ref. [6], for instance the masses and some average quantities. A summary for the  $12^4$  lattice, similar to table 1, is given by table 2.

The main emphasis in the comparison of  $8^4$  to  $12^4$  lattice was put on the behaviour at the phase transition. A study of the time dependence of the average quantities during the updating revealed a clear signal of metastability in a narrow range of  $\kappa$  (in the order of  $\Delta\kappa \approx 10^{-3}$ – $10^{-4}$ ). The resulting two-peak structure of the distribution of the average plaquette was shown in ref. [6]. The time dependence of the average plaquette at ( $\lambda = 1.0$ ,  $\kappa = 0.3041$ ) is given in fig. 4a. One point in the figure represents the average of 200 sweeps, but this averaging is not essential, it was chosen mainly for the better optical presentation. Taking averages over less sweeps (say 50 or 100) gives the same qualitative picture, of course, with larger intrinsic fluctuations within a phase. The two-peak structure of the distribution can also be seen without averaging (the curves become even smoother because of the large number of entries). The two peaks show up also in other average quantities, like average link, average  $\rho$ -link, average length, average action etc. For another example, the time dependence and the distribution of the average link is shown in fig. 4b–4c.

On the  $8^4$  lattice a similar behaviour can be seen near the phase transition at a slightly smaller  $\kappa$ . For instance, the time dependence and distribution of the average link in the point ( $\lambda = 1.0$ ,  $\kappa = 0.3038$ ) is shown by fig. 5a–5b. Although the fluctuations in fig. 5a make an optical impression similar to fig. 4b, the more reliable representation in terms of the distribution in fig. 5b implies that the

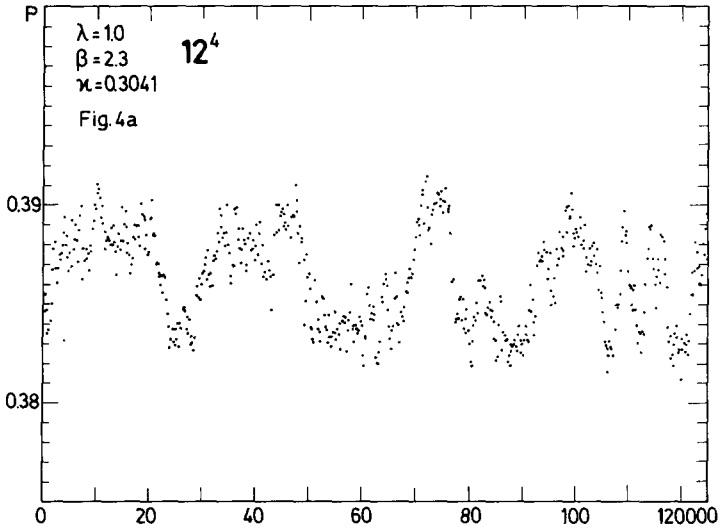


Fig. 4a. The time dependence of average plaquette on a  $12^4$  lattice at ( $\lambda = 1.0$ ,  $\beta = 2.3$ ,  $\kappa = 0.3041$ ). One point represents the average of 200 consecutive sweeps.

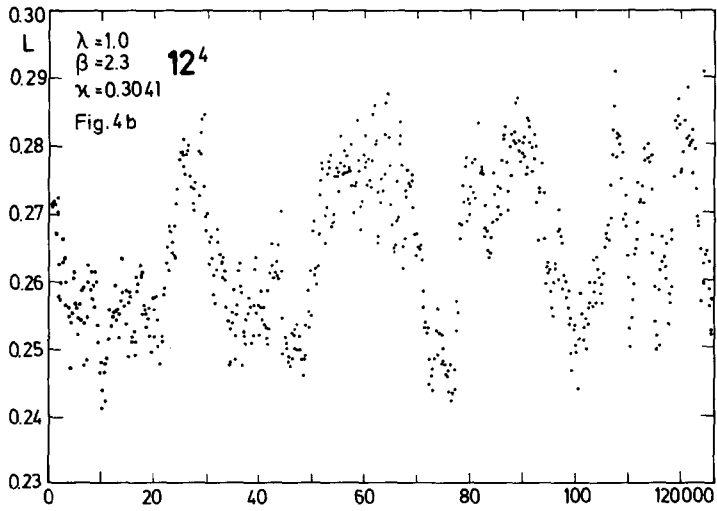


Fig. 4b. The time dependence of average link on a  $12^4$  lattice at ( $\lambda = 1.0$ ,  $\beta = 2.3$ ,  $\kappa = 0.3041$ ). One point represents the average of 200 consecutive sweeps.



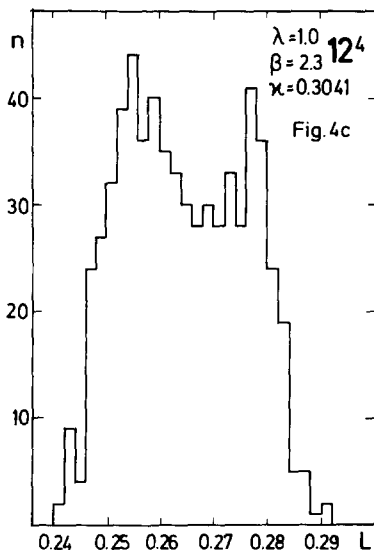


Fig. 4c. The distribution of the points in fig. 4b.

two-state signal is weaker on the  $8^4$  lattice. (In fact, the appearance of several points in table 1 close to each other in  $\kappa$  is the result of a long search for metastability.) Fig. 5b alone would certainly be inconclusive for the existence of two metastable states. Going to a smaller  $\lambda$ -value makes the search for metastability much easier. For instance, the distribution of the average link on the  $8^4$  lattice at ( $\lambda = 0.1$ ,  $\kappa = 0.194$ ) in fig. 5c shows a bump at a low average link. In the time development there is a clear flip to the low value. In fact, we planned this point for the measurement of the couplings, and the metastability was for that purpose an unpleasant surprise. Fig. 5c also shows that the distance of the two peaks is substantially larger at  $\lambda = 0.1$  than at  $\lambda = 1.0$ , that is, for small  $\lambda$  the region of metastability is extending in the average link variable. Therefore, near the phase transition one has to be careful about the judgement of  $\lambda$ -universality, because it can be better in the large volume limit than for a fixed, relatively small, volume. This may explain the “bad”  $\lambda = 0.1$  point for the Higgs mass in fig. 1b.

The lesson from all this is that for the distinction of first versus second-order phase transition one has to (i) tune the coupling parameters very carefully, (ii) collect high statistics (in the range of  $10^5$  sweeps or more), and (iii) use large lattices (with  $10^4$  sites or more). In our opinion, the weaker two-state signal at  $\lambda = \infty$  on the  $12^4$  lattice [6] can be expected to become stronger (and conclusive) on lattices like  $16^4$  or  $20^4$ . Therefore, the confinement-Higgs phase transition is probably first order at  $\beta = 2.3$  for every  $\lambda$ .

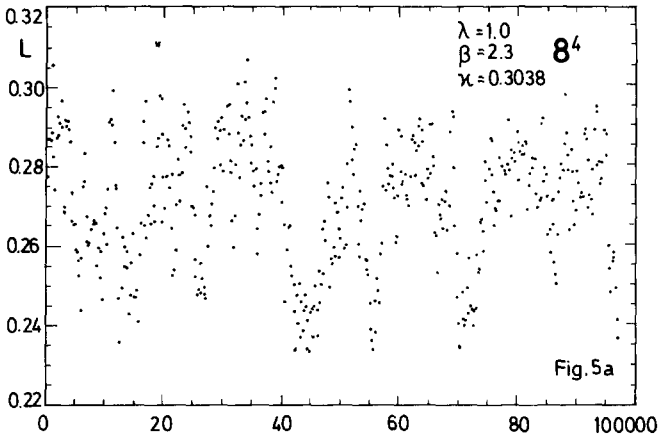


Fig. 5a. The time dependence of average link on a  $8^4$  lattice at ( $\lambda = 1.0$ ,  $\beta = 2.3$ ,  $\kappa = 0.3038$ ). One point represents the average of 200 consecutive sweeps.

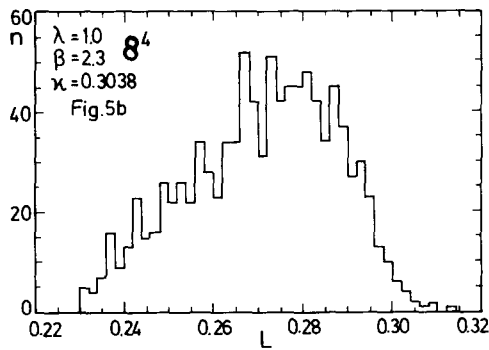


Fig. 5b. The distribution of the points in fig. 5a.

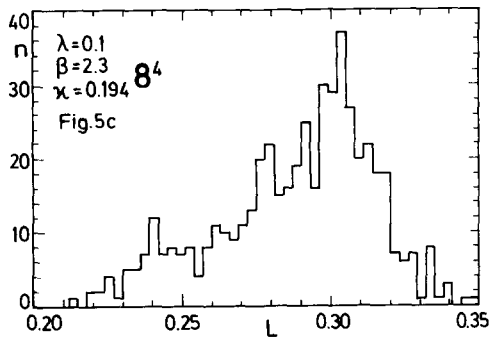


Fig. 5c. The distribution of average link on a  $8^4$  lattice at ( $\lambda = 0.1$ ,  $\beta = 2.3$ ,  $\kappa = 0.194$ ). One entry represents the average of 200 consecutive sweeps.

### 3.3. VOLUME DEPENDENCE OF THE SUSCEPTIBILITY

The critical behaviour near a phase transition can also be investigated by calculating the normalized susceptibility  $\chi_L$  for different lattice sizes  $L$ . The definition of  $\chi_L$  can be

$$\chi_L = \frac{\sum_{\nu} [\langle \text{Tr} V(x, \mu) \text{Tr} V(y, \mu) \rangle - \langle \text{Tr} V(x, \mu) \rangle \langle \text{Tr} V(y, \mu) \rangle]}{\langle [\text{Tr} V(x, \mu)]^2 \rangle - \langle \text{Tr} V(x, \mu) \rangle^2}. \quad (23)$$

Due to the lattice symmetries, this does not depend on  $x$  and  $\mu$ . Another possible definition would be to sum in the numerator over the link directions, too, but as short checks in a few points showed, this does not change any of the qualitative features. Therefore, we used the above definition, which was easier to implement in our programs.

Following the ideas of finite size scaling [11], it is customary to fit the susceptibility  $\chi_L$  on  $L^4$  lattice by the form [12, 13]

$$\chi_L = C \left\{ L^{-2/\nu} + \lambda_2 (\kappa - \kappa_L)^2 \right\}^{2\nu-1}. \quad (24)$$

Here  $\kappa_L$  is the position of the maximum of susceptibility on the  $L^4$  lattice. (It is assumed here, for simplicity, that only the hopping parameter  $\kappa$  changes, the other two couplings  $\lambda$  and  $\beta$  are fixed.) Besides the critical exponent of the correlation length  $\nu < \frac{1}{2}$  there are two arbitrary parameters  $C, \lambda_2$ , which provide a simple parametrization of an arbitrary scaling function.

The data for  $\chi_L$  ( $L = 8, 12$ ) are shown in fig. 6. Besides  $\chi_L$  an analogous quantity in the W-boson channel is also given, which is defined similarly to  $\chi_L$ , only in eq. (23)  $\text{Tr} V$  is replaced everywhere by  $\text{Tr}(\tau V)$ . As one can see, the phase transition influences  $\chi_L$  strongly, but the analogous quantity in the W-channel shows no appreciable structure. Obviously, the phase transition dynamics is dominated by the zero momentum mode in the Higgs boson channel.

For the susceptibility  $\chi_L$  not even a qualitative fit could be achieved by the form in eq. (24). The reason is that the growth of the maximum between  $8^4$  and  $12^4$  would require a critical exponent  $\nu \simeq \frac{2}{5}$  (this corresponds to the roughly linear rise of the maximum with  $L$ ). For such values of  $\nu$ , however, the above form cannot reproduce the general shape of the curves, which have a somewhat flat plateau near the maximum and a rather abrupt decrease. Another functional form we also tried was

$$\chi_L = C \left\{ L^{-4/\nu} + \lambda_4 (\kappa - \kappa_L)^4 \right\}^{\nu-0.5}. \quad (25)$$

This gives a somewhat better description if the asymmetric  $8^4$  points, farther away from the maximum, are omitted from the fit. The  $8^4$  curve shown on fig. 6 belongs

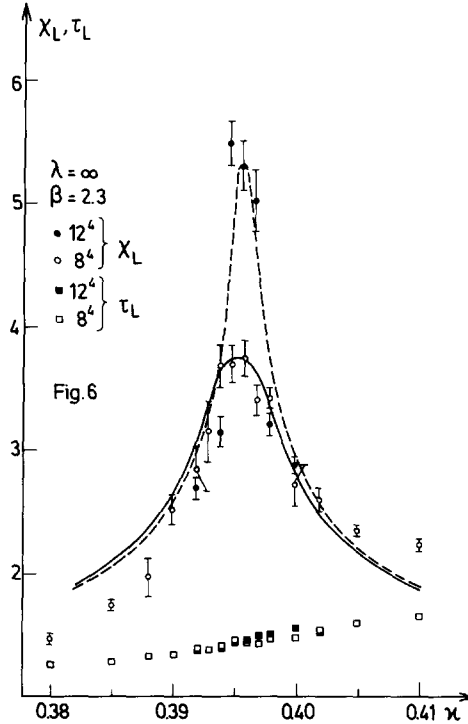


Fig. 6. The susceptibility  $\chi_L$ , defined in eq. (23), for  $L = 8, 12$ . The curves give the best finite size scaling fit we could achieve with the form in eq. (25) (see text). The squares represent an analogous quantity  $\tau_L$  in the W-boson channel, which is defined like  $\chi_L$  in eq. (23), only  $\text{Tr} V$  is replaced everywhere by  $\text{Tr}(\tau V)$ .

to ( $C = 0.6$ ,  $\nu = 0.41$ ,  $\lambda_4 = 80$ ,  $\kappa_8 = 0.3955$ ). This describes the central part of the  $8^4$  points well, but the best choice of  $\kappa_{12} = 0.396$  fails to reproduce the  $12^4$  curve. (The  $\chi^2$  is about 100.) We were unable to find any better simple fit. We are aware of the fact that logarithmic deviations from the above simple forms are expected in dimension four [14], but we do not think that this could explain the observed large deviations. Therefore, our conclusion is that the finite size analysis does not agree with the shape of the susceptibility curves. This is consistent with our expectation that the confinement-Higgs phase transition at  $\beta = 2.3$  is of first order for every  $\lambda$ . Nevertheless, we do not consider the finite size analysis alone decisive. The main argument in favour of the first-order transition comes from the observation of the two-state signal.

Note that the authors of ref. [13] also concluded from their finite size analysis that the phase transition is of first order. Their argument, however, was based mainly on the apparent lack of increase of the maximum between  $L = 4$  and 5. Here one can see, on larger lattices and with much better statistics, that the situation is more subtle because the maximum does increase with  $L$ . Obviously, finite size scaling

ideas are applicable, if at all, only to really large lattices and at the same time good statistics and a reasonable relative change in lattice size is required, in order to see some effect.

#### 4. Weak physical gauge coupling

##### 4.1. HOW TO CHOOSE THE BARE PARAMETERS?

The measured points in the region  $\beta = 2-3$  describe a situation with strong SU(2) gauge coupling at the scale of the W-mass (see, for instance, the discussion in ref. [4]). In the standard electroweak theory the gauge interaction is weak. It would be obviously interesting to perform numerical calculations also in this physically relevant range, particularly in the strong self-coupling region where perturbation theory in  $\lambda$  is not applicable.

The strength of the gauge interaction can be characterized by the coefficient of the Yukawa potential  $\alpha_w$  at distance  $m_w^{-1}$ . This could simply be defined in terms of the derivative of the potential at  $r = m_w^{-1}$ , but later on we shall use a definition which is better suited for a lattice calculation. Specifying the physical distance is, of course, absolutely crucial because the shape of the potential is not purely Yukawa-like. For instance, in QCD with a single quark mass parameter the short-distance potential is known to behave as  $V(r) \sim A/(r \ln(r/\Lambda_c))$ , and therefore it would not make sense to characterize the physical situation by the coefficient of the Coulomb force, unless the distance is fixed. By putting  $r = m_\psi^{-1}$  ( $m_\psi =$  mass of the lowest quark-antiquark bound state) one could, however, uniquely define the physics by the value of  $[r^2 dV/dr]_{r=m_\psi^{-1}}$ . (What is specified here is, of course,  $m_\psi/\Lambda_{\text{lattice}}$ .) Similarly, in the Higgs model one has to fix the distance near  $m_w^{-1}$ . Besides the analogy to QCD with a single heavy quark mass there is, however, also an important difference. Namely, the infrared physics is cut-off in the Higgs phase by the mass of the W-boson, therefore (unlike in QCD) the force between static external charges will never be strong ( $\Lambda_{\text{lattice}}$  is in the Higgs model the scale where the gauge interaction “would become strong” if there were no Higgs mechanism). The absence of the infrared tail makes the numerical MC calculations in the Higgs phase with weak gauge coupling much easier than, say, the corresponding calculations in QCD with a very heavy quark mass ( $m_\psi/\Lambda_{\text{lattice}} \gg 1$ ).

Where could the points in the space of bare parameters be which describe weak gauge interaction at the W-mass scale? We know from previous studies [4] that in the Higgs phase  $\alpha_w$  decreases and  $R_{\text{HW}} \equiv m_{\text{H}}/m_w$  increases if  $\kappa$  is increasing. At the same time  $\mu_w \equiv am_w$  and  $\mu_{\text{H}} \equiv am_{\text{H}}$  are increasing, too, therefore at fixed  $\lambda \sim 1$  and  $\beta \sim 2-3$  it is not possible to reach the small  $\alpha_w$  region, because  $\mu_w$  and  $\mu_{\text{H}}$  will become too large (therefore the lattice artifacts will become dominant). One can, however, simultaneously increase  $\beta$  in order to keep  $\mu_w$  and  $\mu_{\text{H}}$  below, say, 1. The scalar self-coupling  $\lambda$  seems to be irrelevant in the wide range  $1.0 \leq \lambda \leq \infty$ , at

least as far as the limited accuracy of the present Monte Carlo data can tell. Therefore, the value of  $\lambda$  can be fixed for convenience, and only the two relevant parameters  $\beta$ ,  $\kappa$  have to be tuned.

At small distances the coefficient of the Yukawa potential is expected to decrease logarithmically. In a Monte Carlo calculation on very large lattices and with very good accuracy one has to worry about this slow change, too, but in a first exploratory study the sensitivity is usually not good enough, therefore, as a first orientation, the value of  $\alpha_W$  can be taken from a simple potential fit as in ref. [4]. In the present calculation a more detailed investigation below will show a rather weak dependence on the distance, too (see eqs. (35)–(37)). In the standard  $SU(2) \otimes U(1)$  electroweak theory the value of the renormalized  $SU(2)$  coupling  $g_{ren}^2 \equiv 4\pi\alpha_W$  at the scale of the W-boson mass is  $g_{ren}^2 \approx 0.5$ , corresponding to  $\alpha_W \approx 0.04$ . (Here we neglect possible differences due to the different definitions of the renormalized gauge coupling: the couplings are usually defined in momentum space and not by the potential in coordinate space.) In view of  $g_{ren}^{-2} = g^{-2} + o(1)$ , a good first guess is to take  $\beta \equiv 4g^{-2} = 8$  and then try to tune the hopping parameter  $\kappa$  in such a way that  $am_W$  and  $am_H$  be in the measurable range 0.1–1.

A potential difficulty for the numerical calculation is if  $R_{HW}$  becomes too large, because a mass ratio of the order of 10 or more is difficult to control with the presently available computing capacities. A first check at  $\lambda = 1$ ,  $\beta = 8$  and  $\kappa = 0.28$ – $0.32$  on  $10^4$  lattice showed [5] that  $m_H/m_W$  is about 6, which is difficult but seems feasible.

In this section we shall present and discuss the results of a high statistics Monte Carlo calculation at  $\beta = 8$ . For such a high  $\beta$  the inclusion of the gauge degrees of freedom is important, therefore we used the lattice action in eq. (1). Otherwise the calculation was performed in the same way as at  $\beta = 2.3$ . The value of the scalar self-coupling was  $\lambda = 1.0$ . On a  $10^4$  lattice we have chosen the hopping parameter  $\kappa = 0.30$  and performed about  $5 \times 10^4$  full sweeps. We shall refer to this point as point C. The other point is at  $\kappa = 0.28$ , on  $12^4$  lattice, and has about  $2 \times 10^5$  sweeps. This will be called point D. The main emphasis of this first calculation at large  $\beta$  was put on the precise determination of the correlations in as large a spatial volume as possible. This motivates the choice of symmetric lattices, where the correlations between timeslices could be determined after every sweep in all four time orientations. For some questions elongated lattices in the time direction are advantageous, therefore in later calculations with higher statistics such asymmetric lattices should be considered, too. In general, we consider the present calculation only as a first exploratory study. As we shall see, the actual numbers obtained may have large systematic errors on our lattices. The main point we want to make is that the numerical Monte Carlo calculation at high  $\beta$  is not very much more difficult than at  $\beta = 2 - 3$ . The relaxation behaviour of the scalar degrees of freedom is completely normal and is quite similar to the behaviour in the pure  $\phi^4$  model at  $\beta = \infty$ . There is some noticeable rigidity in the gauge degrees of freedom, mani-

fested by a slow drift of expectation values at the scale of a few thousand sweeps, but the amplitude is small even in the long-distance quantities (like large Wilson loops or long-distance correlations). In short, the numerical Monte Carlo investigation of the standard electroweak model with strongly interacting Higgs sector in the physical range of weak gauge couplings is feasible. A possible strategy for future large scale computations in the standard Higgs model is outlined in appendix A.2.

Future Monte Carlo calculations will hopefully allow for some limited change of the lattice spacing, too. In order to follow some singled out renormalization group trajectory (RGT), one has to keep  $\alpha_w$  (or  $m_H/m_w$ ) fixed for decreasing  $am_w$ . If the qualitative picture of the RGT's is given by fig. 3a, then the RGT goes first close to the phase transition and then it goes to  $\beta = \infty$  almost parallel to the phase transition line. In this latter stage the massless RG equation gives a good description of the change of lattice spacing. In the lowest order approximation the lattice spacing  $a$  depends exponentially on  $\beta$ :

$$a\Lambda_{\text{SU}(2)} \simeq \exp\left(-\frac{12}{43}\pi^2\beta\right). \quad (26)$$

Here  $\Lambda_{\text{SU}(2)}$  is the RG invariant  $\Lambda$ -parameter for SU(2). In case of fig. 3b, eq. (26) can still be approximately valid, but then the lattice spacing has a non-zero minimum value, corresponding to the finite  $\beta$  where the singled out RGT ends. Taking, as a first approximation, the mass independent eq. (26) down to  $am_w \simeq 0.1-1$ , we have at  $\beta = 8$

$$m_w/\Lambda_{\text{SU}(2)} \simeq 10^8-10^9. \quad (27)$$

This tells that the infrared scale of the SU(2) gauge coupling, where  $\alpha_w$  would become  $o(1)$  (would there be no Higgs mechanism) is far below the scale of the W-mass. The large ratio in eq. (27) may seem unnatural. In any case, one would like to have an explanation for it.

#### 4.2. YUKAWA POTENTIAL

In order to determine the static energy (in short, ‘‘potential’’) of an external SU(2) doublet charge pair, the Wilson-loop expectation values were calculated in both points at  $\beta = 8$ . The statistics for the Wilson loops was collected in about 8000 sweeps in point C and about 30 000 sweeps in point D on the  $10^4$ , and  $12^4$  lattices, respectively, used also for the measurement of the correlations. Actually, for a more accurate extraction of the large-distance potential elongated lattices would be better suited. From the experience gained in pure gauge theory it is known that a precise measurement of the potential at distance  $R$  requires time extensions  $T \gg R$ . For our present purposes it is, however, enough to know the intermediate distance part of the potential with moderate accuracy. The results for the Wilson loops are summarized in table 3. The potential at lattice-distance  $R$  was extracted from the

TABLE 3  
The expectation values of the Wilson loops  $W_{R,T} = W_{T,R}$  in the two points  
C and D defined in the text

|            | $T = 1$    | $T = 2$     | $T = 3$     | $T = 4$     | $T = 5$     | $T = 6$     |
|------------|------------|-------------|-------------|-------------|-------------|-------------|
| $R = 1$    | 0.90401(1) | 0.83894(2)  | 0.78215(3)  | 0.72991(4)  | 0.68135(4)  | 0.63608(5)  |
| $R = 2, 1$ | 0.90432(2) | 0.75448(4)  | 0.68797(5)  | 0.62942(6)  | 0.57643(7)  | 0.52812(8)  |
| $R = 3, 2$ | 0.83960(5) | 0.75577(9)  | 0.62033(7)  | 0.56290(8)  | 0.51181(9)  | 0.46580(10) |
| $R = 4, 3$ | 0.78311(7) | 0.68984(13) | 0.62301(16) | 0.50827(10) | 0.46043(12) | 0.41776(13) |
| $R = 5, 4$ | 0.73116(8) | 0.63179(14) | 0.56626(19) | 0.51247(23) | 0.41608(14) | 0.37687(16) |
| $R = 6, 5$ | 0.68286(9) | 0.57925(16) | 0.51583(21) | 0.46546(26) | 0.42211(32) | 0.34107(17) |

Entries below the main diagonal refer to the point C ( $10^4$  lattice), the rest gives the result in point D ( $12^4$  lattice). Statistical errors are given in parentheses.

Wilson loops  $W_{R,T}$  by fitting the  $T$ -dependence with two exponentials for  $1 \leq T \leq 5$  on the  $10^4$ , and for  $2 \leq T \leq 6$  on the  $12^4$  lattice. Alternatively, a single exponential fit for  $T \geq 4$  was also performed, in order to reduce the dependence on the small  $T$  region. The numbers given below for the potential were obtained by the first procedure. As the reader can easily check from table 3, the second method gives, within errors the same result, although with somewhat larger errors.

The shape of the potential is expected to be Yukawa-like, corresponding to the massive W-boson exchange. On our lattices the physical potential is, however, distorted by both finite lattice size and finite lattice spacing effects. Since we are in a region of small gauge coupling, these effects can presumably be described (and corrected for) by lowest order perturbation theory. Let us, therefore, briefly consider the Yukawa potential in lattice perturbation theory.

The Yukawa potential in the continuum is generated by the exchange of a massive boson and is proportional to the integral

$$I(r, m) = \int \frac{d^3k}{(2\pi)^3} \frac{e^{ikr}}{k^2 + m^2} = \frac{1}{4\pi r} e^{-mr}, \quad (28)$$

with  $r \equiv |\mathbf{r}|$ . A lattice version is given by

$$I(r, m, a) = \int_{-\pi/a}^{\pi/2} \frac{d^3k}{(2\pi)^3} \frac{e^{ikr}}{\hat{k}^2 + m^2}, \quad (29)$$

where

$$\hat{k}_\mu = \frac{2}{a} \sin \frac{1}{2} k_\mu a. \quad (30)$$

Note that if  $aM$  is the mass determined by the decay of a 2-point function, then in



the propagator one has  $am = 2 \sinh \frac{1}{2} aM$ . If we consider the Wilson-loop in perturbation theory and give the vector boson a mass, then in lowest order we obtain (for  $SU(N)$ )

$$\begin{aligned} V(r) &= - \lim_{T \rightarrow \infty} \frac{1}{aT} \log W_{R,T} = g^2 \frac{N^2 - 1}{2N} \int_{-\pi/a}^{\pi/a} \frac{d^3k}{(2\pi)^3} (1 - e^{ik_3 r}) \frac{1}{\vec{k}^2 + m^2} + o(g^4) \\ &= \text{const} - \alpha_0 \cdot 4\pi \frac{N^2 - 1}{2N} I(r, m, a) + o(g^4) \\ &= \text{const} - \alpha_0 \cdot 3\pi I(r, m, a) + o(g^4). \end{aligned} \quad (31)$$

Here we used  $R \equiv r/a$ ;  $\alpha_0 \equiv g^2/(4\pi)$ , and in the last step we have put  $N = 2$ . The integral in eq. (29) refers to the infinite volume limit. The deviations from the continuum integral give finite  $a$  effects. For small  $a$  we have, keeping  $m, r$  fixed

$$I(r, m, a) = \frac{1}{4\pi r} e^{-mr} \left\{ 1 + \frac{a^2}{4r^2} \left[ 1 + mr + \frac{1}{6} (mr)^3 \right] + o(a^4) \right\}. \quad (32)$$

In our case we have relatively small volumes and large loops, therefore we expect significant finite volume effects. To get an estimate of such effects we consider a finite volume version of  $I(r, m, a)$  (with  $l \equiv aL$  as the physical lattice extension):

$$aI(r, m, a, l) \equiv J(\mu, R, L) = \frac{1}{L^3} \sum_{\mathbf{p} \neq \mathbf{0}} \frac{e^{i\mathbf{p}_3 R}}{\mu^2 + \sum_i 4 \sin^2(\frac{1}{2} p_i)}. \quad (33)$$

Here we have put  $\mu = am$ , and the sum goes over the vectors  $\mathbf{p}$

$$p_i = \frac{2\pi n_i}{L}, \quad n_i = 0, \dots, L - 1. \quad (34)$$

The difference of sums  $J'(\mu, R, L) \equiv J(\mu, R - 1, L) - J(\mu, R, L)$  for  $(\mu = 0.19, L = 12)$ , respectively,  $(\mu = 0.24, L = 10)$  is given in table 4. One can see that for the larger  $R$ -values the finite volume effects are sizeable. The dependence on  $\mu$  is small in this range.

We define an effective  $SU(2)$  gauge coupling on our lattices by

$$\alpha_{SU(2)}(R) \equiv \frac{a}{3\pi} \frac{V(aR) - V(aR - a)}{J'(\mu, R, L)}. \quad (35)$$

From the Monte Carlo data in table 3 we obtain, in point C with  $(\mu = 0.24, L = 10)$  for distances  $R = 2, 3$ , respectively:

$$\text{C: } \alpha_{SU(2)}(R = 2, 3) = 0.0478(5), 0.051(4). \quad (36)$$

TABLE 4  
The finite size dependence of  $J'(\mu, R, L)$  for a few characteristic parameter values

| $R$ | $\mu = 0.19, L = 12$ | $\mu = 0.19, L = 20$ | $\mu = 0.19, L = \infty$ | $\mu = 0.24, L = 10$ | $\mu = 0.24, L = \infty$ |
|-----|----------------------|----------------------|--------------------------|----------------------|--------------------------|
| 2   | 4.168E-2             | 4.170E-2             | 4.171E-2                 | 4.088E-2             | 4.114E-2                 |
| 3   | 1.393E-2             | 1.410E-2             | 1.412E-2                 | 1.315E-2             | 1.369E-2                 |
| 4   | 5.795E-3             | 6.174E-3             | 6.209E-3                 | 4.910E-3             | 5.871E-3                 |
| 5   | 2.551E-3             | 3.224E-3             | 3.275E-3                 | 1.320E-3             | 3.009E-3                 |
| 6   | 7.389E-4             | 1.861E-3             | 1.931E-3                 |                      |                          |

This is somewhat larger than the value reported in ref. [5], because there just a simple Coulomb form was assumed for the short-distance potential. In point D with ( $\mu = 0.19, L = 12$ ), for distances  $R = 2, 3, 4$ , we get

$$D: \alpha_{\text{SU}(2)}(R = 2, 3, 4) = 0.0476(2), 0.0496(12), 0.051(7). \quad (37)$$

These are only slightly  $R$ -dependent and not far from the naive value  $g^2/(4\pi) \simeq 0.040$ . One can also see that, within our errors, there is no difference between the points C and D. From the data at strong gauge coupling it is expected that the exact value at  $R \sim \mu_W^{-1}$  should be slightly smaller in point C than in point D.

#### 4.3. MASS RATIOS AND ZERO MOMENTUM COUPLINGS

For the determination of masses and zero momentum couplings the same quantities were calculated as in the  $8^4$  points discussed in sect. 2. A summary for the  $\beta = 8$  points C and D (defined above), similar to tables 1–3, is given in table 5.

The extraction of the mass in the W-boson channel is straightforward but in the Higgs channel one has to be careful, because the two-W states can also appear. Since on the larger lattice ( $12^4$ ) we have much better statistics, we shall discuss point D in detail and give only the final results in the  $10^4$  point C. A sample of the numerical results for the correlations in point D is given in table 6. The correlations are always normalized by the value of the zero momentum correlation at distance zero. (The sum of the zero momentum correlation over the time slices gives the susceptibility analogous to  $\chi_L$  in eq. (23).)

TABLE 5  
Summary of the masses and average quantities in the two points C and D at  $\beta = 8.0$

| $\lambda$ | $\kappa$ | $am_W$  | $am_H$   | $L$       | $R$       | $P$        | $\rho$    | $s$       |
|-----------|----------|---------|----------|-----------|-----------|------------|-----------|-----------|
| 1.0       | 0.30     | 0.24(2) | 1.39(12) | 0.4652(2) | 0.7048(2) | 0.09568(1) | 1.2004(1) | 6.9214(6) |
| 1.0       | 0.28     | 0.19(1) | 1.21(8)  | 0.3695(1) | 0.5295(1) | 0.09598(1) | 1.1560(1) | 7.2027(2) |

TABLE 6  
Normalized correlations in the point D with  $(\lambda = 1.0, \beta = 8.0, \kappa = 0.28)$

| $d =$       | 0        | 1        | 2        | 3        | 4        | 5        | 6        |
|-------------|----------|----------|----------|----------|----------|----------|----------|
| $C_w^{(2)}$ | 0.871(2) | 0.157(2) | 0.111(2) | 0.097(2) | 0.088(2) | 0.084(1) | 0.082(1) |
| $C_h^{(3)}$ | 2.243(4) | 0.453(3) | 0.139(2) | 0.046(2) | 0.018(2) | 0.010(2) | 0.008(2) |

The zero momentum correlations  $C_w^{(k)}$  obtained by the interpolating fields  $w^{(k)}$  in eq. (7) are strongly dominated by a single low-mass state. The distances  $3 \leq d \leq 6$  can be well fitted by a single exponential:

$$C_w^{(1)}(d) = (0.128 \pm 0.011)\exp\{-d(0.196 \pm 0.016)\} + (d \rightarrow 12 - d),$$

$$C_w^{(2)}(d) = (0.133 \pm 0.013)\exp\{-d(0.196 \pm 0.018)\} + (d \rightarrow 12 - d). \quad (38)$$

The quality of the fits is very good (see, for instance,  $C_w^{(2)}$  in fig. 7). Nevertheless, due to the limitation in time differences, it is not completely excluded that the behaviour for  $3 \leq d \leq 6$  is different from a cosh (for instance, inverse power-like). In

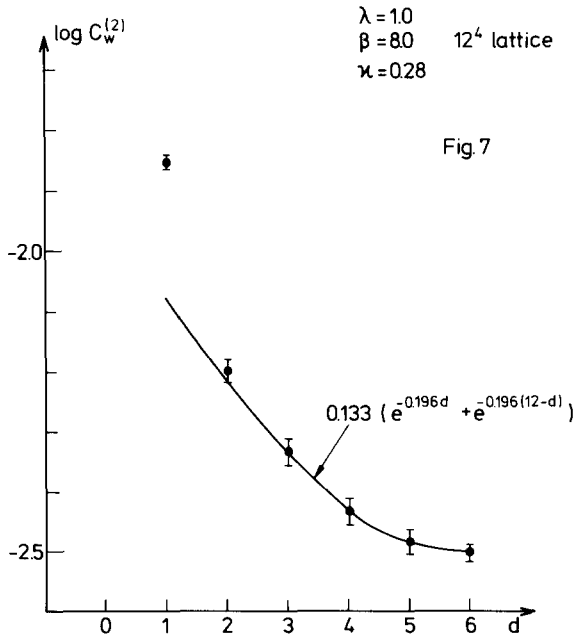


Fig. 7. The correlation  $C_w^{(2)}$  in the W-channel at  $\lambda = 1.0, \beta = 8.0, \kappa = 0.28$  compared to a single cosh fit for distances  $3 \leq d \leq 6$ .

view of fig. 7 we consider this improbable, but a final decision can only be achieved in the future on larger lattices. For the time being we assume that what we see is really the mass gap in the W-channel (otherwise one should go to somewhat larger  $\kappa$ ).

The fit program we used searched for the minimum of the sum of squared deviations divided by the input statistical error squared ( $\chi^2$ ). The errors of the fitted parameters were estimated by treating the input values as independent normally distributed random variables. This is a rather conservative way of error estimation, since the correlations at different distances are obviously strongly correlated with each other (see fig. 7). Alternatively, we also divided the data in 4 bins of 50 000 sweeps and performed the fits in the individual bins. The errors estimated in this way are also consistent with eq. (40). The correlations  $C_w^{(k)}$  can be well fitted by a single mass also for distances  $2 \leq d \leq 6$ , but then the masses are 5–10% higher. This shows that the excited states in the W-channel have either very high mass or are weakly coupled. A two-mass fit for  $1 \leq d \leq 6$  is consistent with a second state about 10–12-times heavier than the lowest state. The  $3 \leq d \leq 6$  fits in the lowest non-zero momentum channel give:

$$\begin{aligned}\bar{C}_w^{(1)}(d) &= (0.076 \pm 0.002) \exp\left\{-d\sqrt{\frac{1}{36}\pi^2 + (0.183 \pm 0.019)^2}\right\} + (d \rightarrow 12 - d), \\ \bar{C}_w^{(2)}(d) &= (0.079 \pm 0.002) \exp\left\{-d\sqrt{\frac{1}{36}\pi^2 + (0.185 \pm 0.020)^2}\right\} + (d \rightarrow 12 - d).\end{aligned}\tag{39}$$

The mass obtained from  $\bar{C}_w^{(k)}$  is practically the same as the one from  $C_w^{(k)}$ , therefore Lorentz invariance is well satisfied. The result for the W-boson mass, together with point C, is

$$\text{C: } am_w = 0.24(2), \quad \text{D: } am_w = 0.19(1).\tag{40}$$

The correlations  $C_h^{(j)}$  of the variables in eq. (6) have a qualitatively different behaviour, because there are clearly at least two masses present. This is shown by a fast decrease at smaller distances and a strong flattening-off at the largest distances. The statistical errors are, unfortunately, still somewhat too large, especially in the correlations of  $h^{(1)}$ , therefore we shall here consider only  $C_h^{(j)}$ , ( $j = 2, 3$ ). The two mass fits for the distances  $1 \leq d \leq 6$  are somewhat unstable due to the large errors. The rough outcome is that there is a strongly coupled high-mass state at  $am \sim 1.2$ – $1.3$  and a very weakly coupled low-mass state with a coupling strength about only 1%. (Correspondingly, the low mass is badly determined.) The mass and the weak coupling to our local variables is consistent with the assumption that the lower state is a 2W-state (see ref. [15]). In order to have tolerable errors from the fit we fixed

the value of the lower state (which we interpret as a 2W-state) and fitted only the remaining 3 parameters. For instance, by fixing the low mass at  $2am_w = 0.38$ , the fit for  $2 \leq d \leq 6$  is:

$$\begin{aligned}
 C_h^{(2)}(d) &= (0.017 \pm 0.009)\exp\{-d \cdot 0.38\} \\
 &\quad + (1.15 \pm 0.12)\exp\{-d(1.22 \pm 0.07)\} + (d \rightarrow 12 - d), \\
 C_h^{(3)}(d) &= (0.031 \pm 0.008)\exp\{-d \cdot 0.38\} \\
 &\quad + (1.55 \pm 0.22)\exp\{-d(1.26 \pm 0.08)\} + (d \rightarrow 12 - d). \quad (41)
 \end{aligned}$$

Varying the fixed lower mass gives the fits in table 7.

The very small values of  $\chi^2$  show that the values of the correlation at different distances are strongly correlated. For  $am_f$  larger than  $2am_w$  the fits become worse, but in the range  $0 \rightarrow 2am_w$  the parameters of the higher state are stable. Masses below  $2am_w$  could have to do with the limited time extension of our lattice (“finite temperature effects”). Taking only the fits with  $am_f \leq 2am_w$ , a somewhat subjective summary of the results is:

$$\text{C: } am_H = 1.39(12), \quad \text{D: } am_H = 1.22(8). \quad (42)$$

In point C the two mass fit is not possible due to the larger errors, nevertheless the flattening-off at the largest distances can still be seen. The value in point C in eq. (42) was obtained from the distances  $1 \leq d \leq 3$ .

If our interpretation of the states in the Higgs-boson channel is correct, then besides the zero relative momentum 2W-state there are also other states to be expected below the high-mass Higgs-boson resonance, namely zero relative momen-

TABLE 7  
 Three parameter fits for  $C_h^{(3)}$ ;  $am_f$  is the fixed lower mass

| $d$   | $am_f$ | $am_H$   | $C_H$    | $C_f$      | $\chi^2$ |
|-------|--------|----------|----------|------------|----------|
| 2 → 6 | 0.00   | 1.20(6)  | 1.47(16) | 0.0030(8)  | 0.008    |
| 2 → 6 | 0.19   | 1.21(6)  | 1.49(18) | 0.0094(26) | 0.008    |
| 2 → 6 | 0.38   | 1.26(8)  | 1.55(22) | 0.031(8)   | 0.02     |
| 2 → 6 | 0.57   | 1.39(14) | 1.70(41) | 0.11(3)    | 0.08     |
| 2 → 6 | 0.76   | 1.83(45) | 2.5(4.7) | 0.34(6)    | 0.37     |
| 1 → 6 | 0.00   | 1.21(2)  | 1.50(3)  | 0.0031(7)  | 0.04     |
| 1 → 6 | 0.19   | 1.21(2)  | 1.50(3)  | 0.0096(23) | 0.02     |
| 1 → 6 | 0.38   | 1.24(3)  | 1.50(3)  | 0.030(7)   | 0.07     |
| 1 → 6 | 0.57   | 1.31(4)  | 1.48(3)  | 0.093(21)  | 0.49     |
| 1 → 6 | 0.76   | 1.43(8)  | 1.35(4)  | 0.28(5)    | 1.67     |

tum multi-W states and also multi-W states with non-zero relative momentum. The resolution of all these states is impossible on our lattice even if higher statistical accuracy would be available. One can expect, however, that the multi-W states are all weakly coupled, similarly to the observed low-mass state, therefore cannot be responsible for the dominant high-mass state. The states with relative momenta are well above the lowest 2W states since  $2\pi/L$  is still relatively large. In future Monte Carlo calculations one has to study the volume dependence of the spectrum on lattices elongated in time, which allow for the better separation of several exponentials. For the theoretical background to the volume dependence of the multi-particle spectrum, including resonances, see ref. [15].

The zero momentum couplings were measured in the same way as for  $\beta = 2.3$ . Here we expect in general smaller couplings. These are, of course, even more difficult to calculate with sufficient precision than the relatively strong couplings at  $\beta = 2.3$ . In point C the  $nH$  couplings disappear completely in the noise. The only useful information we could obtain was for the HWW coupling:

$$\text{C: } a^{-2}\Lambda_{\text{HWW}}^{(k=1)} = 1.56 \pm 0.42, \quad a^{-2}\Lambda_{\text{HWW}}^{(k=2)} = 2.29 \pm 0.41. \quad (43)$$

In point D the situation is slightly better: at least some information for the 3H and 4H couplings could be obtained:

$$\text{D: } l_{3H} = -6.2 \pm 2.8, \quad m_W^{4/3}\rho_{(3)4H} \leq 5. \quad (44)$$

For the HWW coupling the result in point D is:

$$\text{D: } a^{-2}\Lambda_{\text{HWW}}^{(k=1)} = 0.79 \pm 0.32, \quad a^{-2}\Lambda_{\text{HWW}}^{(k=2)} = 1.54 \pm 0.35. \quad (45)$$

This corresponds to an average value  $l_{\text{HWW}} \equiv m_H m_W \Lambda_{\text{HWW}} = 0.27(10)$ , substantially smaller than the value obtained from the tree-level relation  $l_{\text{HWW}} = g_{\text{ren}} = 0.8$ . Assuming pole dominance of the zero-momentum HWW amplitude, the 2W width  $\Gamma_{\text{HWW}}$  of the Higgs boson is given by

$$\frac{\Gamma_{\text{HWW}}}{m_H} = \frac{3m_H^2}{128\pi m_W^2} l_{\text{HWW}}^2 \sqrt{1 - \frac{4m_W^2}{m_H^2}} \left( 1 - \frac{4m_W^2}{m_H^2} + \frac{12m_W^4}{m_H^4} \right) \simeq 0.019. \quad (46)$$

For a Higgs boson mass of  $m_H \simeq 500$  GeV our value of  $l_{\text{HWW}}$  gives a width of about 10 GeV.

## 5. Concluding remarks

Let us briefly summarize the main results of the Monte Carlo calculation:

(i) The approximate  $\lambda$ -independence of the W-boson and Higgs boson mass in the range  $1.0 \leq \lambda \leq \infty$ , if considered as a function of the link expectation value,

turned out to be valid within the present statistical errors (see fig. 1a–1b and also the corresponding fig. 2a–2b for  $12^4$  in ref. [6]).

(ii) The detailed study of the behaviour near the confinement-Higgs phase transition at  $\beta = 2.3$  revealed strong indications of metastability at  $\lambda = 1.0$  and a somewhat weaker two-state signal at  $\lambda = \infty$  (see also ref. [6]). The comparison of the susceptibility on  $8^4$  and  $12^4$  lattices is not consistent with simple finite size scaling. Therefore, the long range Higgs-channel correlations on finite lattices in the phase transition region are presumably due to the metastability associated to first order and not to the critical behaviour associated to second-order phase transition. Our conclusion is that the confinement-Higgs phase transition is probably first order for every  $\lambda$  at finite  $\beta$ , but the strength decreases for increasing  $\lambda$  and/or  $\beta$ .

(iii) The zero-momentum  $n$ -Higgs-boson couplings are numerically difficult to obtain. Because of the large statistical errors the present results can only be considered as upper limits in absolute value. The zero-momentum Higgs-WW coupling turned out to be measurable and does not show strong  $\lambda$ -dependence between  $\lambda = 1.0$  and  $\lambda = 0.1$ .

(iv) A high-statistics Monte Carlo calculation at weak physical gauge coupling, roughly equal to the weak SU(2) coupling in the standard SU(2)  $\otimes$  U(1) electroweak theory, showed that a numerical investigation at strong self-coupling and weak gauge coupling is feasible. The chosen value  $\lambda = 1.0$  of the scalar self-coupling is in the non-perturbative range, where the non-perturbative feature of  $\lambda$ -independence is expected. (In fact, the observed  $\lambda$ -independence at  $\beta = 2.3$  and  $\beta = \infty$  strongly suggests a similar  $\lambda$ -independence at  $\beta = 8$ , too.) The  $2 \times 10^5$  sweeps on a  $12^4$  lattice allowed the separation of two distinct states in the Higgs boson channel: a weakly coupled state with roughly twice the W-mass and a strongly coupled high-mass state with

$$\frac{m_H}{m_W} = 6.4 \pm 0.8. \quad (47)$$

Our interpretation for the low-mass state, based on the comparison to the low- $\beta$  points, is that it is a zero relative momentum  $2W$ -state, therefore the Higgs-W mass ratio is as given by eq. (47). (Future careful studies of the volume dependence of the spectrum may clear up the origin of the low-mass state.) The W-boson channel is dominated by the lowest state. The next excited W-state has a 10–12 times higher mass. For the  $n$ -Higgs couplings we only obtained upper bounds in absolute value, but the zero-momentum Higgs-WW coupling turned out to be measurable. Its value is roughly by a factor of 3 smaller than the naive application of the tree-level formulas would give. Therefore, the width of the high-mass Higgs boson can be reasonably small, unless decays into multi-W channels dominate. All our  $\beta = 8$  results could still contain considerable finite size effects, because the correlation length in the W-channel is only slightly less than the half of the lattice extension.

The effect of the finite time extension (“finite temperature effects”) may also be important. Further Monte Carlo calculations on larger lattices (e.g.  $12^3 \times 36$ ,  $16^4$  or  $20^4$ ) should be performed in order to determine the magnitude of these “systematic errors” in eq. (47). Because of these uncertainties it is not yet possible to draw the final conclusion about the Higgs mass to W-mass ratio at the given coupling constant values.

We consider the calculation at  $\beta = 8.0$  in the present paper only as a first exploratory study. The important point is the *possibility* of MC calculations in the strongly self-interacting standard Higgs model with weak gauge coupling. Future numerical studies could, however, go much further. A possible strategy of an “ideal” large scale MC calculation in the standard Higgs model is outlined in appendix A.2. The main information obtained from such a calculation would be the functional relation between different physical quantities in the non-perturbative self-coupling regime. For a phenomenologically realistic calculation the Yukawa- and gauge-couplings to the fermions have to be included, too. Taking all the foreseeable difficulties into account, we believe that a Monte Carlo calculation with 10% error in the non-perturbative  $\lambda$  regime of the standard  $SU(2) \otimes U(1)$  model is easier than the Monte Carlo calculation of the proton mass in QCD with 1% accuracy.

In order to have a firm theoretical interpretation of the Monte Carlo data, one has also to do more analytic work. The numerical calculation is necessarily restricted to relatively small cut-off’s. The extension of the conclusions to higher cut-off’s requires that numerical calculations be performed also in the validity range of an analytic expansion. In particular, a small gauge coupling expansion around the critical line  $\kappa_{cr}(\lambda)$  ( $\lambda$  fixed) of the  $\phi^4$  model at  $\beta = \infty$  should be done [16].

All our Monte Carlo data are consistent with the expectation that (at least for large enough  $\lambda$  and  $\beta$ ) the pattern of the RGT’s is qualitatively given either by fig. 3a or by fig. 3b. The first would be the case if the confinement-Higgs phase transition would be second order, or if the maximum correlation length at the first-order transition would increase sufficiently fast for  $\beta \rightarrow \infty$ . This would imply the existence of a non-perturbative non-trivial  $\lambda$ -independent continuum limit, in the mathematical sense, at the  $\beta = \infty$  critical point for sufficiently large  $\lambda$ . In the second case no exact continuum limit would exist, suggesting a fundamental difference between elementary fermion and scalar matter fields. Due to the bounded correlation length at the first-order phase transition, the RGT’s would end on the discontinuity for finite lattice spacing (i.e. for finite cut-off). Of course, if the maximum cut-off would be very high, the distinction would not be important from the practical point of view. In the case of a non-perturbative non-trivial  $\lambda$ -independent continuum limit the Higgs mass could, in principle, be predicted from the W-mass and the strength of the gauge coupling. Unfortunately, the MC calculations are unable to decide the question of the existence of such a continuum limit.



We are indebted to W. Hollik, M. Lüscher and T.T. Wu for helpful discussions.

## Appendix A

### A.1. RGT'S OR CCP'S

The notion of renormalization group trajectories (RGT's) in the general case of several independent couplings was introduced in the earlier literature on field theory and statistical physics [17,18]. Still it seems to us useful to recollect here the definitions in the specific context of lattice regularization, in order to make clear what do we precisely mean in the discussion of the continuum limit.

Let us consider a lattice field theory with  $n$  coupling parameters  $[g] \equiv g_1, g_2, \dots, g_n$ . In order to define the RGT's or "curves of constant physics" (CCP's) in the space of coupling parameters, let us choose a "reference quantity"  $m_1$  with physical dimension of mass. Its value in lattice units  $\mu_1 = am_1$  is a function of the couplings:  $\mu_1 = \mu_1[g]$ . In addition let us choose  $(n - 1)$  independent, dimensionless ratios of physical quantities:  $[\xi] \equiv \xi_2, \xi_3, \dots, \xi_n$ , and consider the "curves of constant reference ratios"  $C_{[\xi]}$  with  $\xi_k = \text{const}(k = 2, 3, \dots, n)$ . Along such curves the change of the reference quantity  $\mu_1 = am_1$  defines the change of the lattice unit  $a$  uniquely. An absolute value of  $a$  in terms of some physical units (e.g.  $eV^{-1}$ ) is specified if the physical value of  $m_1$  as a function of  $[\xi]$  is given. A simple possibility is to take the value of  $m_1$   $[\xi]$ -independent, but other choices can be sometimes more advantageous. (One has to keep in mind, that for  $m_1 = [\xi]$ -independent the absolute scale on  $C_{[\xi]}$  depends on the choice of the reference quantity.) On a given curve  $C_{[\xi]}$  the coupling constants  $g_i$  ( $i = 1, \dots, n$ ) can be considered as functions of the lattice spacing:  $g_i = g_i^{[\xi]}(a)$ , and the corresponding  $\beta$ -function can be defined as

$$\beta_i[g] \equiv -a \frac{dg_i^{[\xi]}(a)}{da}. \quad (\text{A.1})$$

Sometimes it is also convenient to choose a reference coupling, say,  $g_1$  and consider, on a given curve  $C_{[\xi]}$ , the lattice spacing and the other couplings as a function of it:  $a = a^{[\xi]}(g_1)$  and  $g_k = g_k^{[\xi]}(g_1)$  ( $k = 2, 3, \dots, n$ ). In this case one has, obviously

$$\frac{dg_k^{[\xi]}}{dg_1} = \frac{\beta_k[g]}{\beta_1[g]}. \quad (\text{A.2})$$

This can be considered as a differential equation for the curves of constant reference ratios.

The necessary condition for the existence of a continuum limit is, that there exists (at least one) “critical point”  $[g_c] = g_{1c}, g_{2c}, \dots, g_{nc}$  in the coupling space, such that

(i)  $[g_c]$  lies on some subset  $R_c$  of the curves of constant reference ratios;

(ii) for  $C_{[\xi]} \in R_c$  we have  $\lim_{g_1 \rightarrow g_{1c}} a^{[\xi]}(g_1) = 0$ ;

(iii) every (in general dimensionful) physical quantity  $P$  measured on the lattice tends on  $C_{[\xi]} \in R_c$  for  $[g] \rightarrow [g_c]$  to a  $[\xi]$ -dependent value  $P_c^{[\xi]}$  in such a way, that the deviation from the limiting value vanishes at least as fast as some integer power of  $\mu_1$  (or of  $a$ ).

In other words, physical quantities are constant along  $C_{[\xi]} \in R_c$  in the vicinity of the critical point  $[g_c]$  up to corrections (“lattice artifacts”) of order at most  $\mu_1$ . It is useful to define a “scaling region”  $S_c$  belonging to  $[g_c]$  by the requirement that the deviation of physical quantities from the continuum limit  $P_c^{[\xi]}$  is in some specified sense “small” for  $[g] \in S_c$ . Within the scaling region  $S_c$  the curves  $C_{[\xi]}$  can simply be called “curves of constant physics” (CCP’s). Since dimensionless ratios of physical quantities are, apart from small scaling violations, constant in the scaling region, the CCP’s are, within these small lattice artifacts, independent of the choice of the set of reference quantities. Because of the above mentioned freedom in defining the scale, it is natural to consider the dimensionful physical quantities as functions of the lattice spacing  $a$  and of the couplings  $[g]$ :  $P = P(a, g_1, \dots, g_n)$ . In the scaling region  $S_c$  the constancy of the physical quantities along the CCP’s can be expressed by the “renormalization group equation” (RGE):

$$\left\{ -a \frac{\partial}{\partial a} + \sum_{i=1}^n \beta_i[g] \frac{\partial}{\partial g_i} \right\} P = o(\mu_1). \quad (\text{A.3})$$

Here the r.h.s. stands for the “scaling violating” lattice artifacts. This equation reflects the fact, that in the scaling region the change in lattice spacing can be compensated (up to lattice artifacts) by an appropriate change (“renormalization”) in the couplings. Therefore, the CCP’s can also be called RGT’s.

In a general situation one cannot expect that there is only a single critical point in the coupling parameter space. The “critical set” consisting of all critical points may contain subsets describing completely different continuum physics. A singled out critical subset belonging to a unique continuum theory can also consist of more than one point. For instance, if some combination of the coupling parameters is “irrelevant”, the critical point can occur for different values of this irrelevant combination. The number of “relevant” variables belonging to a given unique critical subset is very important, because it gives the number of independent physical parameters in the continuum theory. For simplicity, let us now only consider the situation, where every point in the critical set defines the same continuum theory. For a precise definition of the number of relevant couplings let us consider the  $(n - 1)$ -dimensional hypersurface  $H_{\mu_1}$ , where the value of the reference quantity is equal to  $\mu_1$ . As a

function of  $\mu_1$ , the values of the reference ratios  $[\xi]$  on  $H_{\mu_1}$  define a one-parameter family  $V_{\mu_1}$  of subsets in the space of possible values of reference ratios. The number of relevant couplings ( $n - l$ ) is defined as the dimensionality of  $V_{\mu_1}$  in the limit  $\mu_1 \rightarrow 0$ . (The number of irrelevant couplings is, of course,  $l$ .) Another possible (equivalent) definition is obtained if one considers, for given continuum values  $[\xi_0]$  of the reference ratios and for some small  $\varepsilon$ , the region  $\Lambda_\varepsilon[\xi_0]$  in the coupling space, where the deviation of the reference ratios from  $[\xi_0]$  is small:  $|\xi_k - \xi_{0k}| < \varepsilon$ , ( $k = 2, 3, \dots, n$ ). If the section  $W_{\varepsilon\mu_1}[\xi_0] = H_{\mu_1} \cap \Lambda_\varepsilon[\xi_0]$  for  $\varepsilon, \mu_1 \rightarrow 0$  has dimension  $l$ , then the number of irrelevant couplings is  $l$ . (These two criteria for the relevance of couplings will be referred to later on as “first” and “second” criterium, respectively.)

It is interesting to consider, what happens with those curves  $C_{[\xi]}$ , where the values of the reference ratios are not equal to some possible set of values in the continuum limit. (These curves are outside the subset  $R_c$  considered in the above definition of a critical point.) First of all, it is enough to consider only the subspace, say,  $\bigcup_{\mu_1 \leq 1} V_{\mu_1}$ , because the points where the reference mass in lattice units is larger than 1 is of little interest for the continuum limit. If in this subspace there are still curves  $C_{[\xi]}$  outside  $R_c$ , then these curves can either end on the boundary with  $\mu_1 = 1$  or on the boundary of the parameter space (some of the couplings can become, for instance, infinite), or they can end on a discontinuity inside the parameter space. Such discontinuities can be produced, for instance, in the infinite volume limit by a first order phase transition.

It follows from the above definition that for the study of the continuum limit the irrelevant couplings can be omitted or kept constant. The RGE will be valid with  $(n - l)$  instead of  $n$  couplings. A critical point  $[g_c]$  with  $(n - l)$  relevant couplings can be said to have “rank”  $(n - l)$ .

It is possible that the above requirement (iii) for a critical point is fulfilled only for some well defined subset  $Q_c$  of physical quantities. (For instance,  $P \in Q_c$  is allowed to depend only on some subset of field variables.) Such a critical point can be called “reduced”. The number of relevant couplings for a reduced critical point is usually smaller (its rank is lower) than for a normal critical point.

Let us now apply these definitions, for example, to the case of the possible continuum limit of the standard Higgs model as conjectured in ref. [4]. Since in this case there are 3 couplings  $(\lambda, \beta, \kappa)$ , we have  $n = 3$ . The set of critical points of interest is the line  $(\lambda, \kappa_{cr}(\lambda))$  at  $\beta = \infty$ . The critical points may be equivalent to the  $\lambda = \infty$  point for every  $\lambda > 0$  or, perhaps, only for sufficiently large  $\lambda > \lambda_0$ . In the following we shall only consider the subset equivalent to  $\lambda = \infty$ . As the reference quantity one can choose the W-mass:  $\mu_1 \equiv \mu_W = am_W$ . For one of the dimensionless quantities one can take  $\xi_2 \equiv R_{HW} = m_H/m_W$ . For the other one let us choose the coefficient of the Yukawa potential  $\xi_3 \equiv \alpha_W$  at distance  $m_W^{-1}$ . (This can be defined, for instance, by eq. (35) with  $R \approx \mu_W^{-1}$ .) The fixing of the physical distance is, of course, very important because at small physical distances the coefficient of the

potential is expected to decrease. If in the continuum limit at the  $\beta = \infty$  critical line there is one irrelevant coupling, then for the above second criterium one has to consider the regions  $W_{\varepsilon\mu_W}[R_{HW}, \alpha_W]$ , where  $\mu_W$  is small and the deviation of  $R_{HW}$  and  $\alpha_W$  from the correct continuum limit value is small. In the limit  $\mu_W \rightarrow 0$  and vanishing deviation  $\varepsilon \rightarrow 0$  this region has to be one-dimensional. A simple realization of this would be the  $\lambda$ -independence of the physical quantities for fixed expectation values of the gauge invariant link variable, because then  $W_{\varepsilon\mu_1}[R_{HW}, \alpha_W]$  would have a one-dimensional limit. Of course, the limited accuracy of the present MC calculations ( $\varepsilon$  and  $\mu_W$  are not very small) does not really allow for a strong conclusion. The observed crude  $\lambda$ -independence can, however, be considered as a first hint for the irrelevance of the self-coupling  $\lambda$ . Assuming the existence of a  $\lambda$ -independent non-trivial continuum limit at  $\lambda, \kappa_{cr}(\lambda)$ , ( $\lambda > \lambda_0$ ), it follows from the above first criterium of relevance that the Higgs mass to W-mass ratio  $R_{HW}$  is uniquely determined if  $\alpha_W$  is given. In other words, the Higgs mass is not a free parameter as it seems to be in perturbation theory. Every CCP where this relation between  $\alpha_W$  and  $R_{HW}$  is not satisfied has to end on the boundary or on some discontinuity and has, therefore, a minimum lattice spacing (maximum cut-off).

Returning again to the general case, the definition of CCP's does not necessarily require the existence of true critical points with infinite correlation lengths (i.e.  $a \rightarrow 0$ ). It is very well possible that in the vicinity of some point with very large (but finite) correlation length the long distance physical quantities show an approximate scaling behaviour. In this case the CCP's or RGT's, the number of relevant couplings etc. can be defined as before. An example is the scaling behaviour represented by fig. 3b. Compared to the  $\beta = \infty$  critical point of rank two in fig. 3a, the difference is that in fig. 3b the one-parameter manifold of CCP's does not reach  $\beta = \infty$  but, depending on one of the relevant parameters, ends somewhere on the first order discontinuity. The  $\lambda$ -independence (for large enough  $\lambda$ ) remains in this case presumably only approximate. Considering the whole 3-dimensional coupling parameter space, there is a two-parameter family of CCP's ending on the discontinuity. The  $\beta = \infty$  critical line has in this case only one relevant parameter. In the Higgs phase it is a trivial free theory of massive W-bosons. Going to the  $\beta = \infty$  critical line from the confining phase ( $\kappa < \kappa_{cr}$ ), one has presumably a reduced critical point with one relevant coupling equivalent to pure SU(2) gauge theory.

## A.2. AN IDEAL MONTE CARLO CALCULATION IN THE STRONGLY INTERACTING STANDARD HIGGS MODEL

Let us now describe a MC calculation in the standard Higgs model under generous assumptions concerning computer time and storage. Namely, we shall assume good statistical accuracy of the measured masses, coupling constants, potentials etc. in the range of correlation lengths between 1 and 10 lattice units. In addition, the possibility of reliable MCRG studies of the RG trajectories up to correlation lengths like 40 or 80 will be assumed.

The MC calculation consists of two stages. In the first stage the reference quantities  $\mu_W = am_W$  (W-mass),  $R_{HW} = m_H/m_W$  (Higgs mass to W-mass ratio) and  $\alpha_W$  (the coefficient of the Yukawa potential at distance  $m_W^{-1}$ , which is defined by eq. (35) with  $R \approx \mu_W^{-1}$ ) are measured, together with other physical quantities like coupling constants etc. One can concentrate the measured points on the surface  $\alpha_W = 0.04$ , corresponding to the physical strength of the Yukawa potential in the standard  $SU(2) \otimes U(1)$  model. Due to the limitation  $0.1 \leq \mu_W, \mu_H \leq 1$  the points have to be within some strip on this surface. It has to be expected that there is a limitation of measurability also at small  $\lambda$ -values. Up to now the high-statistics MC calculations were restricted to the range  $0.1 \leq \lambda \leq \infty$ . This region may perhaps be extended to still smaller  $\lambda$ -values, for instance by more sophisticated updating procedures, but the flatness of the effective potential in the Higgs field length will somewhere set a lower limit:  $\lambda \geq \lambda_{\min}$ .

The main physical information obtained from the Monte Carlo calculations is contained in the functional relations between different physical quantities in the “measurable strip”. As an example, let us consider the Higgs-WW coupling  $l_{HWW}$ . A possible outcome of the MC calculation is illustrated in fig. 8a for fixed reference mass (for instance,  $\mu_W = 0.2$ ). The interesting part of the figure is the region of non-perturbative self-coupling (NP), where low-order perturbation theory in  $\lambda$  is not valid, therefore the MC calculation can provide us new information. It would be nice, if the lower limit  $\lambda_{\min}$  of the measurable strip would be such that some overlap between the validity of lattice perturbation theory and of the MC calculations could be found.

The second stage of the MC calculation is the study of scaling along the curves of constant physics (CCP’s). To some extent this can be done by changing the scale within the measurable strip. For instance, Fig. 8a has to be the same (apart from small scale breaking “lattice artifacts”) also for  $\mu_W = 0.1$ . For very large correlation lengths, however, the long-distance physical quantities are very difficult to measure. Fortunately, one can follow the CCP’s (or RGT’s) with MCRG methods based on some other quantities which satisfy the RG equations: generalized Creutz-ratios of Wilson-loops or block-spin expectation values etc. The result can be that some CCP’s end for correlation lengths which are too small for a reasonable quasi-continuum effective theory. A minimum requirement could be, for instance, that the maximum correlation length in the W-channel be at least  $\sim 50$  (corresponding to  $\mu_{W\min} < 0.02$ , or in physical units to a cut-off  $> 4$  TeV). Those points in fig. 8a where the corresponding CCP does not satisfy this requirement should be discarded (dashed piece of the curve). The rest of the curve describes respectable quasi-continuum effective theories, which are of interest even if the strict continuum limit is trivial.

A favourable situation would be that every measured point would satisfy the minimum requirement for a sensible quasi-continuum effective theory. Moreover, if there were a non-trivial true continuum limit, some points of the curve in fig. 8a

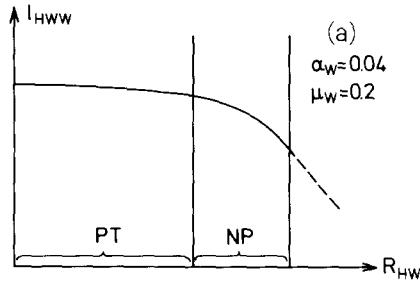


Fig. 8a. The functional relation between the Higgs-WW coupling constant  $l_{HWW}$  and the Higgs-W mass ratio  $R_{HW}$ . PT is the regime of perturbation theory, NP is the non-perturbative region where MC calculations are particularly interesting. The dashed piece of the curve is in the region, where the maximum correlation length on the corresponding CCP is smaller than some reasonable lower bound (say,  $(\mu_{\bar{W}}^1)_{\max} < 50$ ).

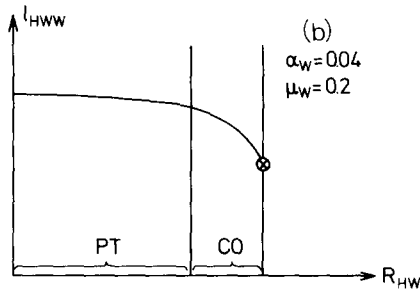


Fig. 8b. The picture corresponding to fig. 8a in the case of a  $\lambda$ -independent non-trivial continuum limit. The perturbative regime is denoted also here by PT. There is a non-perturbative cross-over region (CO) with finite maximum cut-off, which leads to the unique point ( $\otimes$ ) corresponding to the continuum theory.

would correspond to a CCP with infinite maximum correlation length. What would be the picture if there were a  $\lambda$ -independent non-trivial continuum limit (with 2 relevant parameters), as conjectured in ref. [4]? (In this case the CCP's in the  $\lambda = \text{const}$  planes, at least for sufficiently large  $\lambda$  and  $\beta$ , would look like fig. 3a.) As it is depicted in fig. 8b, every point on the curve  $l_{HWW}(R_{HW})$  would correspond to a finite maximum cut-off (the corresponding CCP's would end on the first-order phase transition surface in the intermediate  $\lambda$  range), except for the endpoint ( $\otimes$ ). This unique point would correspond to the continuum theory characterized by a unique relation between  $\alpha_W$ ,  $R_{HW}$  and  $l_{HWW}$ . In this case every MC calculation in the scaling region with sufficiently large  $\lambda$  (say,  $\lambda \geq 1.0$ ) would give this unique relation. Unfortunately, the question about the *existence* of the  $\lambda$ -independent continuum limit cannot be answered by numerical MC calculations, which are limited to rather modest values of the correlation lengths.

## References

- [1] K.G. Wilson, *Phys. Rev. D*10 (1974) 2445
- [2] J. Fröhlich, *in Progress in gauge field theory, Cargèse lecture, 1983*, ed. G. 't Hooft et al. (Plenum, 1984)
- [3] J. Jersák, *Lattice Higgs models*, talk given at the Wuppertal Workshop on Lattice Gauge Theory, Aachen preprint PITHA 85/25 (November 1985)
- [4] I. Montvay, *Nucl. Phys. B*269 (1986) 170; DESY preprint 85-005 (1985)
- [5] I. Montvay, *in Advances in lattice gauge theory, Proc. 1985 Tallahassee Conference*, ed. D.W. Duke, J.F. Owens (World Scientific, 1985)
- [6] W. Langguth and I. Montvay, *Phys. Lett.* 165B (1985) 135
- [7] D.J.E. Callaway and R. Petronzio, *Nucl. Phys. B*267 (1986) 253
- [8] J. Jersák, C.B. Lang, T. Neuhaus and G. Vones, *Aachen preprint PITHA 85/05* (1985)
- [9] M.M. Tsypin, *Lebedev Institute, Moscow preprint no. 280* (1985)
- [10] E. Brézin and J. Zinn-Justin, *Nucl. Phys. B*257 [FS14] (1985) 867
- [11] M.E. Fisher, *in Critical phenomena, Proc. 51st Enrico Fermi Summer School, Varenna, 1970*, ed. M.S. Green (Academic Press, New York, 1972);  
M.N. Barber, *in Phase transitions and critical phenomena, vol. VIII.*, ed. C. Domb, J. Lebowitz (Academic Press, New York, 1984)
- [12] B. Lautrup and M. Nauenberg, *Phys. Lett.* 95B (1980) 63
- [13] M. Tomiya and T. Hattori, *Phys. Lett.* 140B (1984) 370
- [14] E. Brézin, *J. Phys.* 43 (1982) 15
- [15] M. Lüscher, *DESY preprint 86-034* (1986)
- [16] I. Montvay, *Phys. Lett.* 172B (1986) 71
- [17] K.G. Wilson and J. Kogut, *Phys. Reports* 12C (1974) 75
- [18] E. Brézin, J.C. Le Guillou and J. Zinn-Justin, *in Phase transitions and critical phenomena*, ed. C. Domb, M.S. Green (Academic Press, London, 1976) vol. 6, p. 125